

Limits of reinforcement learning for decision trees in Markov decision processes

Anonymous authors
Paper under double-blind review

Keywords: Reinforcement learning, decision trees, POMDP

Summary

The summary appears on the cover page. Although it can be identical to the abstract, it does not have to be. One might choose to omit the stated contributions in the Summary, given that they will be stated in the box below. The original abstract may also be extended to two paragraphs. The authors should ensure that the contents of the cover page fit entirely on a single page. The cover page does **not** count towards the 8–12 page limit.

 Lorem ipsum dolor sit amet, consectetur adipiscing elit. Ut purus elit, vestibulum ut, placerat ac, adipiscing vitae, felis. Curabitur dictum gravida mauris. Nam arcu libero, nonummy eget, consectetur id, vulputate a, magna. Donec vehicula augue eu neque. Pellentesque habitant morbi tristique senectus et netus et malesuada fames ac turpis egestas. Mauris ut leo. Cras viverra metus rhoncus sem. Nulla et lectus vestibulum urna fringilla ultrices. Phasellus eu tellus sit amet tortor gravida placerat. Integer sapien est, iaculis in, pretium quis, viverra ac, nunc. Praesent eget sem vel leo ultrices bibendum. Aenean faucibus. Morbi dolor nulla, malesuada eu, pulvinar at, mollis ac, nulla. Curabitur auctor semper nulla. Donec varius orci eget risus. Duis nibh mi, congue eu, accumsan eleifend, sagittis quis, diam. Duis eget orci sit amet orci dignissim rutrum.

Contribution(s)

1. Provide a succinct but precise list of the contribution(s) of the paper. Use contextual notes to avoid implications of contributions more significant than intended and to clarify and situate the contribution relative to prior work (see the examples below). If there is no additional context, enter “None”. Try to keep each contribution to a single sentence, although multiple sentences are allowed when necessary. If using complete sentences, include punctuation. If using a single sentence fragment, you may omit the concluding period. A single contribution can be sufficient, and there is no limit on the number of contributions. Submissions will be judged mostly on the contributions claimed on their cover pages and the evidence provided to support them. Major contributions should not be claimed in the main text if they do not appear on the cover page. Overclaiming can lead to a submission being rejected, so it is important to have well-scoped contribution statements on the cover page.

Context: None

2. The submission template for submissions to RLJ/RLC 2026

Context: Built from previous RLC/RLJ, ICLR, and TMLR submission templates

3. *[Example of one contribution and corresponding contextual note for the paper “Policy gradient methods for reinforcement learning with function approximation” (?).]*

This paper presents an expression for the policy gradient when using function approximation to represent the action-value function.

Context: Prior work established expressions for the policy gradient without function approximation (?).

Limits of reinforcement learning for decision trees in Markov decision processes

Anonymous authors

Paper under double-blind review

Abstract

For applications like medicine, machine learning models ought to be interpretable. In that case, models like decision trees are preferred over neural networks because humans can read their predictions from the root to the leaves. Learning such decision trees for sequential decision making problems is a relatively new research direction and most of the existing literature focuses on imitating (or distilling) neural networks. In contrast, we study reinforcement learning (RL) algorithms that *directly* return decision trees optimizing some trade-off of cumulative rewards and interpretability in a Markov decision process (MDP). We show that such algorithms can be seen as learning policies for partially observable Markov decision processes (POMDPs). We use this parallel to understand why in practice it is often easier to use imitation learning than to learn the decision tree from scratch for MDPs.

1 Introduction

Interpretability in machine learning is commonly divided into local and global approaches Gianois et al. (2024). Local methods—also referred to as explainability or post-hoc methods Lipton (2018)—provide explanations for individual predictions using tools such as local linear approximations Ribeiro et al. (2016), saliency maps Puri et al. (2020), feature attributions Lundberg & Lee (2017), or attention mechanisms Shi et al. (2022). Although widely used, these methods approximate the behavior of an underlying black-box model and may therefore be unfaithful to its true computations Atrey et al. (2020).

Global interpretability approaches instead restrict the model class so that the learned model is transparent by construction. Decision trees Breiman et al. (1984) are a canonical example, as their predictions can be inspected, reasoned about, and formally verified. This makes them particularly attractive for safety-critical applications and has motivated extensive research in supervised learning Murthy & Salzberg (1995); Verwer & Zhang (2019); Demirovic et al. (2022); Demirović et al. (2023); van der Linden et al. (2023).

Extending global interpretability to sequential decision making, however, remains challenging. Existing approaches largely rely on *indirect* methods Milani et al. (2024): a high-performing but opaque policy (typically a neural network) is first learned using reinforcement learning, and an interpretable model is then trained to imitate its behavior. A prominent example is VIPER Bastani et al. (2018), which distills neural network policies into decision trees using imitation learning Ross et al. (2010). Such methods have demonstrated strong empirical performance and enable formal verification Wu et al. (2024), but they optimize a surrogate objective—policy imitation—rather than the original reinforcement learning objective. As a result, the best decision tree policy for the task may differ substantially from the tree that best approximates a neural expert. The curious reader will find an example of this phenomenon in the appendix 8.

This limitation motivates the study of *direct* approaches that learn interpretable policies by optimizing the reinforcement learning objective itself. While direct decision tree learning is well understood

38 in supervised settings, it is far less developed for sequential decision making. Understanding why
39 direct optimization is difficult—and when it can succeed—is the central focus of this work.
40 In this article, we show that reinforcement learning of decision tree policies for MDPs, i.e. learning
41 a decision tree that directly optimizes the cumulative reward of the process without relying on a
42 black-box expert, is often very difficult. To do so, we construct very simple MDPs for which we
43 know optimal decision tree policies and show that RL consistently fails to retrieve those policies.
44 We identify partial observability as a key reason for those failures.
45 In section 2, we present the related work on reinforcement learning to train decision tree policies for
46 MDPs. In section 3, we present key concepts for decision trees, MDPs, and the formalism of Topin
47 et al. (2021) for reinforcement learning of decision tree policies. In section 4, we show that this
48 direct approach is equivalent to learning a *deterministic memoryless* policy for partially observable
49 MDP (POMDP) Sondik (1978) which is a hard problem Littman (1994). In section 5, we present
50 our methodology to benchmark RL algorithms that train decision tree policies. In section 5.3, we
51 show that when RL fails to retrieve optimal decision tree policies for MDPs it is most likely because
52 partial observability is involved.

53 2 Related work

54 There exist reinforcement learning algorithms that directly train decision tree policies optimizing
55 the cumulative rewards in a given MDP. These approaches can be divided into methods based on
56 *parametric* and *non-parametric* trees.
57 Parametric decision trees fix the tree structure *a priori*—including depth, node arrangement, and
58 selected state features—and only learn the decision thresholds. This formulation enables differentia-
59 bility and allows direct optimization of the RL objective using policy gradient methods Sutton
60 et al. (1999). Several works Silva et al. (2020); Vos & Verwer (2024); Marton et al. (2025) employ
61 PPO to train such differentiable trees. While these methods can achieve strong performance, they
62 require the tree structure to be specified in advance, making it difficult to adaptively trade off inter-
63 pretability and performance. An overly complex structure may require post-hoc pruning, whereas
64 an insufficiently expressive structure may fail to represent good policies. Moreover, Marton et al.
65 (2025) reports that additional stabilization techniques, such as adaptive batch sizes, are often nec-
66 essary for direct reinforcement learning to match indirect imitation methods Bastani et al. (2018)
67 performances. Non-parametric decision trees, by contrast, are the standard model in supervised
68 learning, where algorithms efficiently construct trees that balance predictive performance and inter-
69 pretability Breiman et al. (1984); Bertsimas & Dunn (2017). This trade-off is optimized by using a
70 regularized training objective. However, training non-parametric trees to trade-off MDP cumulative
71 rewards and interpretability is largely unexplored Milani et al. (2024). To the best of our knowledge,
72 the only work that studies this setting: Topin et al. (2021). Topin et al. introduce *iterative bound-
73 ing MDPs* (IBMDPs), which augment the downstream MDP with additional state features, actions,
74 rewards, and transitions. They show that certain policies in the IBMDP correspond to decision tree
75 policies for the downstream MDP. Hence, standard RL algorithms can be used to learn such policies
76 in IBMDPs. Finally, a few specialized methods exist for restricted problem classes. For maze-like
77 MDPs, Mansour et al. (2022) proves the existence of optimal decision tree policies and provides
78 a constructive algorithm. In settings where the MDP model is fully known, Vos & Verwer (2023)
79 use planning to compute shallow parametric decision tree policies. Next, we recall useful technical
80 material.

81 3 Technical preliminaries

82 3.1 Markov decision processes

83 Markov decision processes were first introduced in the 1950s by Richard Bellman Bellman (1957).
84 Informally, an MDP models how an agent acts over time to achieve a goal. At every time step,

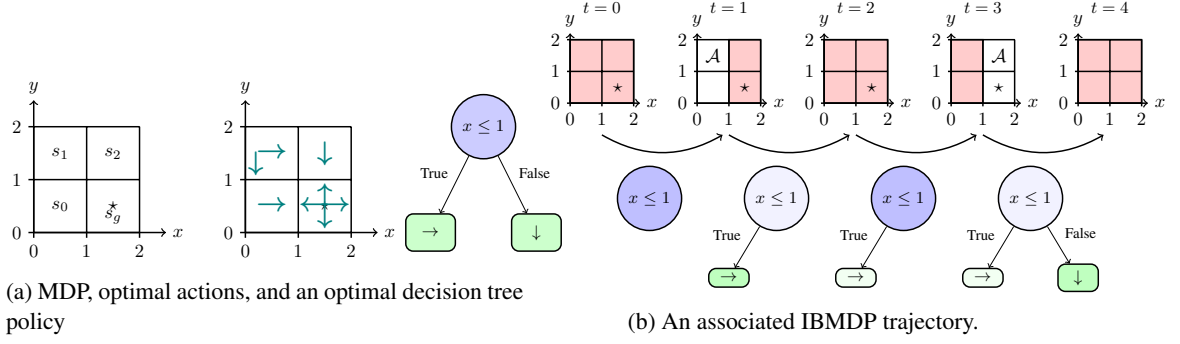


Figure 1: On the left of figure 1a, a grid world MDP with, four states, four directional actions that moves an agent, and rewards of 0 for every transitions except when taking an action in the bottom right goal state (\star). The states have discrete labels that represent their coordinates in the $[0, 2] \times [0, 2]$ square, e.g. for s_0 , $x = 0.5$, $y = 0.5$. In the centre, an optimal actions w.r.t the RL objective (definition 2). On the right, an optimal depth-1 decision tree policy w.r.t the RL objective (definition 2) that takes a state label as input, performs some tests on the state coordinate, and returns a directional action. On figure 1b, an IBMDP trajectory when the downstream MDP is the grid world from figure 1a. In the top row, we graphically represent what the IBMDP state at a given time t , and in the bottom row, we present the corresponding decision tree policy traversal. When the pink covers the whole grid, the information contained in the observation o_t could be interpreted as ‘the current state features could be anywhere in the grid’. The more information-gathering actions are taken, the more refined the bounds on the current downstream state features get. At $t = 0$, the downstream state features are $s_0 = (0.5, 1.5)$ and the initial observation is always the downstream MDP default state feature bounds (definition 5): $o_0 = (0, 2, 0, 2)$ because the downstream state features are in $[0, 2] \times [0, 2]$. This means that the overall IBMDP state is $s_{IB} = (0.5, 1.5, 0, 2, 0, 2)$. The first action is an IGA $\langle x, 1 \rangle$ that tests the feature x of the downstream state against the value 1 and the reward is ζ (definition 5). This transition corresponds to going through an internal node $x \leq 1$ in a decision tree policy as illustrated in the figure. At $t = 1$, after gathering the information that the x -value of the current downstream state is below 1, the observation is updated with the refined bounds $o_1 = (0, 1, 0, 2)$, i.e. more information has been gathered and the obstructed pink area shrinks. The downstream state features remain unchanged. The agent then takes a downstream action that is to move right. This gives a reward 0, resets the observation to the original downstream state feature bounds, and changes the features to $s_2 = (1.5, 1.5)$. And the trajectory continues like this until the absorbing downstream state $s_4 = (1.5, 0.5)$ is reached. By masking the current downstream state features to an agent, we would force it to take information-gathering actions otherwise it would not know how to act optimally (figure 1a).

85 the agent observes its current state (e.g., patient weight and tumor size) and takes an action (e.g.,
 86 administers a certain amount of chemotherapy). The agent receives a reward that helps evaluate the
 87 quality of the action with respect to the goal (e.g., tumor size decrease when the objective is to cure
 88 cancer). Finally, the agent transitions to a new state (e.g., the updated patient state) and repeats this
 89 process over time:

90 **Definition 1** (Markov decision process). An MDP is a tuple $\mathcal{M} = \langle S, A, R, T, T_0 \rangle$. S is a finite
 91 set of states representing all possible configurations of the environment. A is a finite set of actions
 92 available to the agent. $R : S \times A \rightarrow \mathbb{R}$ is a deterministic reward function that assigns a real-
 93 valued reward to each state-action pair. While in general reward functions are often stochastic, in
 94 this manuscript we focus deterministic ones without loss of generality. $T : S \times A \rightarrow \Delta(S)$ is the
 95 transition function that maps state-action pairs to probability distributions over next states $\Delta(S)$.
 96 $T_0 \in \Delta(S)$ is the initial distribution over states.

97 Informally, we would like to act in an MDP so that we obtain as much reward as possible over time.
 98 We can formally define this objective, that we call the reinforcement learning objective, as follows:

99 **Definition 2** (Reinforcement learning objective). Given an MDP (definition 1) $\mathcal{M} \equiv$
 100 $\langle S, A, R, T, T_0 \rangle$, the goal of reinforcement learning for sequential decision making is to find a model,
 also known as a policy, $\pi : S \rightarrow A$ that maximizes the expected discounted sum of rewards:

$$J(\pi) = \mathbb{E} \left[\sum_{t=0}^{\infty} \gamma^t R(s_t, \pi(s_t)) \mid s_0 \sim T_0, s_{t+1} \sim T(s_t, \pi(s_t)) \right]$$

99 where $0 < \gamma \leq 1$ is the discount factor that controls the trade-off between immediate and future
 100 rewards.

101 Algorithms presented in this article aim to find an optimal policy $\pi^* \in \operatorname{argmax}_{\pi} J(\pi)$ that maximizes
 102 the above reinforcement learning objective. In particular, RL algorithms Sutton & Barto (1998);
 103 Sutton et al. (1999); Watkins & Dayan (1992); Mnih et al. (2015); Schulman et al. (2017) learn
 104 such optimal policies using data of MDP interactions without prior knowledge of the reward and
 105 transition models. Useful quantities for such algorithms include *value* of states and actions.

106 **Definition 3** (Value of a state). In an MDP \mathcal{M} (definition 1), the value of a state $s \in S$ under policy
 107 π is the expected discounted sum of rewards starting from state s and following policy π :

$$V^\pi(s) = \mathbb{E} \left[\sum_{t=0}^{\infty} \gamma^t R(s_t, \pi(s_t)) \mid s_0 = s, s_{t+1} \sim T(s_t, \pi(s_t)) \right]$$

108 Applying the Markov property gives a recursive definition of the value of s under policy π :
 109 $V^\pi(s) = R(s, \pi(s)) + \gamma \mathbb{E}[V^\pi(s') \mid s' \sim T(s, \pi(s))]$. The optimal value of a state $s \in S$, $V^*(s)$,
 110 is the value of state s when following the optimal policy π^* (the policy that maximizes the RL
 111 objective (definition 2)): $V^*(s) = V^{\pi^*}(s)$. Similarly, the optimal value of a state-action pair
 112 $(s, a) \in S \times A$, $Q^*(s, a)$, is the value when taking action a in state s and then following the optimal
 113 policy: $Q^*(s, a) = R(s, a) + \gamma \mathbb{E}[V^*(s') \mid s' \sim T(s, a)]$.

114 3.2 Decision tree policies

115 While other interpretable policy classes exist Kohler et al. (2025b), one conjecture from Glanois
 116 et al. (2024) is that interpretable models are all hard to optimize or learn because they are non-
 117 differentiable in nature. This is something that will be key in our study of decision tree policy that
 118 we introduce next.

119 **Definition 4** (Decision tree policy). A decision tree policy is a rooted tree $\pi_T = (\mathcal{N}, E)$. Each
 120 internal node $v \in \mathcal{N}$ is associated with a test that maps an MDP state attribute to a Boolean, e.g.
 121 $s_i \leq v$ for $v \in \mathbb{R}$. Each edge $e \in E$ from an internal node corresponds to an outcome of the
 122 associated test function. Each leaf node $l \in \mathcal{N}$ is associated with an MDP action $a_l \in A$. For any
 input $s \in S$, the tree defines a unique path from root to leaf, determining the prediction $\pi_T(s) = a_l$
 where l is the reached leaf. The depth of a tree is the maximum path length from root to any leaf.

123 In figure 1a, we present an example Markov decision process (definition 1), the optimal actions
 124 that maximize the RL objective (definition 2), and a decision tree policy (definition 4) that also
 125 maximizes the RL objective. Next, we present the class of MDPs introduced in Topin et al. (2021)
 126 useful for our to understand reinforcement learning of decision tree policies that directly optimize
 127 the RL objective in an MDP.

128 **3.3 Iterative bounding Markov decision processes**

129 The key thing to know about iterative bounding Markov decision processes (IBMDPs) is that they
 130 are, as their name suggests, MDPs (definition 1). Hence, IBMDPs admit an optimal deterministic
 131 Markovian policy that maximizes the RL objective Bellman (1957). From now on, we will assume
 132 that all the MDPs we consider are MDPs with continuous state spaces and a finite set of actions,
 133 and we use bold fonts for states and observations as that are vector-valued. However all our results
 134 generalize to discrete states (in \mathbb{Z}^m) MDPs that we can factor using one-hot encodings. Given an
 135 MDP for which we want to learn a decision tree policy—the downstream MDP–IBMDP states are
 136 concatenations of the downstream MDP state features and some observations. Those observations
 137 are information about the downstream state features that are refined—‘iteratively bounded’—at each
 138 step. Those observations essentially represent some knowledge about where some downstream state
 139 features lie in the state space. Actions available in an IBMDP are: (i) the actions of the downstream
 140 MDP, that change downstream state features, and (ii) *information-gathering* actions (IGAs) that
 141 change the aforementioned observations. Now, downstream actions in an IBMDP are rewarded like
 142 in the downstream MDP, this ensures that the RL objective w.r.t. the downstream MDP is encoded in
 143 the IBMDP reward. When taking an information-gathering action, the reward is an arbitrary value
 144 such that optimizing the RL objective in the IBMDP is equivalent to optimizing some trade-off
 145 between interpretability and the RL objective in the downstream MDP. Before showing how to get
 146 decision tree policies from IBMDP policies, we give a formal definition of IBMDPs following Topin
 147 et al. (2021):

148 **Definition 5** (Iterative bounding Markov decision process (Topin et al. (2021), section 4.1)). Given
 149 a downstream MDP $\mathcal{M} \equiv \langle S, A, R, T, T_0 \rangle$ (definition 1), an associated iterative bounding Markov
 150 decision process \mathcal{M}_{IB} is a tuple:

$$\langle \overbrace{S \times O}^{\text{State space}}, \overbrace{A \cup A_{info}}^{\text{Action space}}, \overbrace{(R, \zeta)}^{\text{Reward}}, \overbrace{(T_{info}, T, T_0)}^{\text{Transitions}} \rangle$$

151 S are the downstream MDP state features. Downstream state features $s = (s_1, \dots, s_p) \in S$
 152 are bounded: $s_j \in [L_j, U_j]$ where $\infty < L_j \leq U_j < \infty \forall 1 \leq j \leq p$. O are observa-
 153 tions. They represent bounds on the downstream state features: $O \subsetneq S^2 = [L_1, U_1] \times \dots \times$
 154 $[L_p, U_p] \times [L_1, U_1] \times \dots \times [L_p, U_p]$. So the complete IBMDP state space is $S \times O$: the
 155 concatenations of downstream state features and observations. Given some downstream state fea-
 156 tures $s = (s_1, \dots, s_p) \in S$ and some observation $o = (L_1, U_1, \dots, L_p, U_p)$, an IBMDP state
 157 is $s_{IB} = (\underbrace{s_1, \dots, s_p}_{\text{downstream state features}}, \underbrace{L_1, U_1, \dots, L_p, U_p}_{\text{observation}})$. A are the downstream MDP actions. A_{info}
 158 are *information-gathering* actions of the form $\langle j, v \rangle$ where j is a state feature index $1 \leq j \leq p$
 159 and v is a real number between L_j and U_j . So the complete action space of an IBMDP is the set
 160 of downstream MDP actions and information-gathering actions $A \cup A_{info}$. $R : S \times A \rightarrow \mathbb{R}$ is
 161 the downstream MDP reward function. ζ is a reward signal for taking an information-gathering
 162 action. So the IBMDP reward function is to get a reward from the downstream MDP if the ac-
 163 tion is a downstream MDP action or to get ζ if the action is an IGA action. $T_{info} : S \times$
 164 $O \times (A_{info} \cup A) \rightarrow \Delta(S \times O)$ is the transition function of IBMDPs: given some observation
 165 $o_t = (L'_1, U'_1, \dots, L'_p, U'_p) \in O$ and downstream state features $s_t = (s'_1, s'_2, \dots, s'_p)$ if an IGA
 166 $\langle j, v \rangle$ is taken, the new observation o_{t+1} is $(L'_1, U'_1, \dots, L'_j, \min\{v, U'_j\}, \dots, L'_p, U'_p)$ if $s_j \leq v$ or
 167 $(L'_1, U'_1, \dots, \max\{v, L'_j\}, U'_j, \dots, L'_p, U'_p)$ if $s_j > v$. If a downstream action is taken, the observa-
 168 tion is reset to the default downstream state feature bounds $(L_1, U_1, \dots, L_p, U_p)$ and the downstream
 169 state features change according to the downstream MDP transition function: $s_{t+1} \sim T(s_t, a_t)$.

170 At initialization, the downstream state features are drawn from the downstream MDP initial dis-
171 tribution T_0 and the observation is always set to the default downstream state features bounds
172 $\mathbf{o}_0 = (L_1, U_1, \dots, L_p, U_p)$.

173 We present an IBMDP for a the grid-world MDP (figure 1a) in figure 1b. Now remains to extract a
174 decision tree policy (definition 4) for a downstream MDP \mathcal{M} from a policy for an associated IBMDP
175 \mathcal{M}_{IB} .

176 **3.4 From policies to trees**

177 information-gathering actions (definition 5) resemble the tests $1_{\{x_{-j} \leq v\}}$ that make up internal de-
178 cision tree nodes (figure 1b). Indeed, a policy taking actions in an IBMDP essentially builds a tree
179 by taking sequences of IGAs (internal nodes) and then a downstream action (leaf node) and repeats
180 this process over time. In particular, the IGA rewards ζ can be seen as a regularization or a penalty
181 for interpretability: if ζ is very small compared to downstream rewards, a policy will try to take
182 downstream actions as often as possible, i.e. build shallow trees with short paths between root and
183 leaves.

184 Topin et al. (2021) show that not all IBMDP policies are decision tree policies for the downstream
185 MDP. In particular, their algorithm that converts IBMDP policies into decision trees (algorithm 1)
186 takes as input deterministic policies depending solely on the observations of the IBMDP. If the poli-
187 cies were not deterministic, different subtrees could stem from similar IBMDP observations: this
188 means that the corresponding policy would be a stochastic decision tree Blanc et al. (2021). While
189 there is nothing wrong in learning stochastic decision tree policies from a performance standpoint,
190 interpreting a stochastic policy is an open problem that is not our focus. If the policies were depend-
191 ing on the current full IBMDP state rather than solely on the current IBMDP observation, then a
192 learning agent has 0 incentive to take information-gathering actions to build a decision tree policy as
193 all the state information required to optimally control the downstream MDP as well as downstream
194 actions are available to the agent (definition 5 and figure 1b). The connections between partially
195 observable MDPs (POMDPs Sondik (1978); Sigaud & Buffet (2013)) and extracting decision tree
196 policies from IBMDPs might seem obvious but they are absent from the original IBMDP paper Topin
197 et al. (2021) and from subsequent work. In the next section we bridge this gap.

198 **4 Bridging the gap with the partially observable MDPs literature**

199 **4.1 An adequate formalism**

200 To better understand reinforcement learning of decision tree policies for MDPs, we explicitly re-
201 write the problem of optimizing a deterministic policy depending on current observations in an
202 IBMDP as the problem of optimizing a deterministic policy depending only on current observations—
203 also known as a deterministic *memoryless* policy—in a partially observable Markov decision process
204 (POMDP Sondik (1978)). By doing so, we can leverage results from the POMDP literature that is
205 richer than interpretable reinforcement learning literature.

206 **Definition 6** (Partially observable Markov decision process). A partially observable Markov de-
207 cision process is a tuple $\langle X, A, O, R, T, T_0, \Omega \rangle$. X is the hidden state space. A is a finite set
208 of actions. O is a set of observations. $T : X \times A \rightarrow \Delta(X)$ is the transition function, where
209 $T(\mathbf{x}_t, a, \mathbf{x}_{t+1}) = P(\mathbf{x}_t | \mathbf{x}_{t+1}, a)$ is the probability of transitioning to state \mathbf{x}_t when taking action a
210 in state \mathbf{x} . T_0 : is the initial distribution over states. $\Omega : X \rightarrow \Delta(O)$ is the observation function,
211 where $\Omega(o, a, \mathbf{x}) = P(o | \mathbf{x}, a)$ is the probability of observing o in state \mathbf{x} . $R : X \times A \rightarrow \mathbb{R}$ is the
212 reward function, where $R(\mathbf{x}, a)$ is the immediate reward for taking action a in state \mathbf{x} . Note that
213 $\langle X, A, R, T, T_0 \rangle$ defines an MDP (definition 1).

214 Next, we can define partially observable iterative bounding Markov decision processes (POIB-
215 MDPs). They are IBMDPs (definition 5) for which we explicitly define an observation space and an
216 observation function.

217 **Definition 7** (Partially observable iterative bounding Markov decision process). a partially observ-
 218 able iterative bounding Markov decision process \mathcal{M}_{POIB} is a tuple:

$$\underbrace{\langle S \times O, A \cup A_{info}, \Omega \rangle}_{\text{States}}, \underbrace{(R, \zeta)}_{\text{Observations}}, \underbrace{(T_{info}, T, T_0)}_{\text{Rewards}}, \underbrace{\Omega}_{\text{Transitions}}$$

219 , where $\langle S \times O, A \cup A_{info}, (R, \zeta), (T, T_0, T_{info}) \rangle$ is an IBMDP (definition 5). The transition
 220 function Ω maps concatenation of state features and observations–IBMDP states–to observations,
 221 $\Omega : S \times O \rightarrow O$, with $P(o|(s, o)) = 1$

222 POIBMDPs are particular instances of POMDPs where the observation function simply applies a
 223 mask over some features of the hidden state. This setting has other names in the literature. For
 224 example, POIBMDPs are mixed observability MDPs Araya-López et al. (2010) with downstream
 225 MDP state features as the *hidden variables* and feature bounds as *visible* variables. POIBMDPs can
 226 also be seen as non-stationary MDPs (N-MDPs) Singh et al. (1994) in which there is one different
 227 transition function per downstream MDP state: these are called hidden-mode MDPs Choi et al.
 228 (2001). Following Singh et al. (1994) we can write the value of a deterministic memoryless policy
 229 $\pi : O \rightarrow A \cup A_{info}$ in observation o .

230 **Definition 8** (Value of an observation). In a POIBMDP (definition 7), the expected cumulative dis-
 231 counted reward of a deterministic memoryless policy $\pi : O \rightarrow A \cup A_{info}$ starting from observation
 232 o is $V^\pi(o)$: $V^\pi(o) = \sum_{(s, o') \in S \times O} P^\pi((s, o')|o) V^\pi((s, o'))$. With $P^\pi((s, o')|o)$ the asymptotic
 233 occupancy distribution (see section 4 from Singh et al. (1994) for the full definition) of the hidden
 234 POIBMDP state (s, o') given the partial observation o and $V^\pi((s, o'))$ the classical state-value func-
 235 tion (definition 3). We abuse notation and denote both values of observations and values of states by
 236 V since the function input is not ambiguous.

237 4.2 Reinforcement learning in POMDP

238 In general, the policy that maximizes the RL objective (definition 2) in a POMDP (definition 6) maps
 239 “belief states” or observation histories to actions Sigaud & Buffet (2013). Hence, those policies do
 240 not correspond to decicion trees since we require that policies depend only on the current observation
 241 (algorithm 1). If we did not have this constraint, we could apply any standard RL algorithm to solve
 242 POIBMDPs by seeking policies depending on belief states or observations histories because those
 243 are sufficient to optimally control any POMDP Sigaud & Buffet (2013); Lambrechts et al. (2025a).

244 In particular, the problem of finding the optimal deterministic memoryless policies for POMDPs is
 245 NP-HARD, even with full knowledge of transitions and rewards(section3.2 from Littman (1994)).
 246 It means that it is impractical to enumerate all possible policies and take the best one. For even
 247 moderate-sized POMDPs, a brute-force approach would take a very long time since there are $|A|^{|O|}$
 248 deterministic memoryless policies. Hence it is interesting to study reinforcement learning for finding
 249 the best deterministic memoryless policy since it would not enumerate the whole solution space.

250 In Singh et al. (1994), the authors show that the optimal memoryless policy can be stochastic. Hence,
 251 policy gradient algorithms Sutton et al. (1999)–that return stochastic policies–are to avoid since we
 252 seek the best *deterministic* policy. Furthermore, the optimal deterministic memoryless policy might
 253 not maximize all the values of all observations simultaneously Singh et al. (1994) which makes it
 254 difficult to use TD-learning algorithms like Q-learning Watkins & Dayan (1992). Indeed, doing
 255 a TD-learning update of one observation’s value (definition 8) can change the value of *all* other
 256 observations in an uncontrollable manner because of the dependence in $P^\pi((s, o')|o)$ (definition 8).

257 Despite those hardness results, applying RL to POMDPs, by naively replacing the processes (hidden)
 258 states x by the observation o in Q-learning or Sarsa Sutton & Barto (1998), has already demonstrated
 259 successful in practice Loch & Singh (1998). More recently, the framework Baisero et al. (2022);
 260 Baisero & Amato (2022) called asymmetric RL, has also shown promising results to learn policies
 261 for POMDPs. Asymmetric RL algorithms train a model–a policy or a value function–depending

on hidden state (only available at train time) and a history dependent (or observation dependent) model. The history or observation dependent model serves as target or critic to train the hidden state dependent model. The history dependent (or observation dependent) model can thus be deployed in the POMDP after training since it does not require access to the hidden state to output actions. In appendix 12 we present asymmetric variants of standard tabular RL algorithm. For example, asymmetric Q-learning is a variant of Q-learning that returns a deterministic memoryless policy. Given a POMDP, asymmetric Q-learning trains a partially observable Q-function $Q : O \times A \rightarrow \mathbb{R}$ and a Q-function $U : X \times A \rightarrow \mathbb{R}$. The hidden state dependent Q-function U serves as a target in the temporal difference learning update. It is the tabular version of the modified DQN algorithm used in Topin et al. (2021). Indeed, when learning deterministic memoryless policies for IBMDPs, Topin et al. (2021) were using RL algorithms corresponding to asymmetric DQN or asymmetric PPO from Baisero et al. (2022); Baisero & Amato (2022) before those were published. We provide a reproducibility study in appendix 9 of Topin et al. (2021). In appendix 12, we describe tabular asymmetric variants such as asymmetric Q-learning, which learns an observable Q-function $Q : O \times A \rightarrow \mathbb{R}$ using a hidden-state target $U : X \times A \rightarrow \mathbb{R}$. This mirrors the modified DQN approach used in Topin et al. (2021), which effectively applied asymmetric DQN/PPO before these frameworks were formalized. We also provide a reproducibility study of Topin et al. (2021) in appendix 9. Until recently, the benefits of asymmetric RL over standard RL was only shown empirically and only for history-dependent models. The work of Lambrechts et al. (2025b) proves that some asymmetric RL algorithms should in theory learn better history-dependent **or** memoryless policies for POMDPs. This is exactly what we wish for. However, those algorithms are not practical because they require estimations of the asymptotic occupancy distribution $P^\pi((s, o')|o)$ (definition 8) for candidate policies which in turn would require to perform costly Monte-Carlo estimations. We leave it to future work to use those algorithms that combine asymmetric RL and estimation of future visitation frequencies since those results are contemporary to the writing of this manuscript.

287 5 Methodology

288 The goal of this section is to check if the aforementioned approach can consistently retrieve optimal
289 decision tree policies for a simple grid world MDP (figure 1a). In particular, we use reinforcement
290 learning to train decision tree policies for MDPs by seeking deterministic memoryless policies that
291 optimize the RL objective in POIBMDPs (figure 1b and section 4).

292 5.1 Computing some decision tree policies

293 To assess the performance of reinforcement learning, for different trade-off reward ζ (definition 5),
294 we identify the deterministic memoryless policies that maximize the RL objective (definition 2).
295 Each of those policies correspond to one of the decision tree policies for the grid world downstream
296 MDP illustrated in figure 2: (i) a depth-0 tree equivalent to always taking the same downstream
297 action ($\pi_{\mathcal{T}_0}$), (ii) a depth-1 tree equivalent alternating between an IGA and a downstream action
298 ($\pi_{\mathcal{T}_1}$), (iii) an unbalanced depth-2 tree that sometimes takes two IGAs then a downstream action
299 and sometimes a an IGA then a downstream action ($\pi_{\mathcal{T}_u}$), (iv) a depth-2 tree that alternates between
300 taking two IGAs and a downstream action ($\pi_{\mathcal{T}_d}$), or (v) an infinite ‘tree’ that only takes IGAs. We
301 will particularly focus on trying to retrieve the depth-1 decision tree that is the most interpretable–
302 smallest number of nodes and shallowest–tree taking optimal actions. Because from Singh et al.
303 (1994) we know that for POMDPs, stochastic memoryless policies can sometimes get better ex-
304 pected discounted rewards than deterministic memoryless policies, we also compute the value of
305 the stochastic policy that randomly alternates between two downstream actions: \rightarrow and \downarrow . Taking
306 those two downstream actions always lead to the goal state in expectation (figure 1a). Because we
307 know all the downstream states, all the observations, all the actions, all the rewards and all the trans-
308 sitions of our POIBMDPs, we can compute the RL objective values of those different deterministic
309 memoryless policies exactly given ζ and γ a discount factor. We plot, in figure 2, the RL objec-
310 tive values of the decision tree policies as functions of ζ when we fix $\gamma = 0.99$ (standard choice
311 of discount in practice Sutton & Barto (1998)). Despite objective values being very similar for the

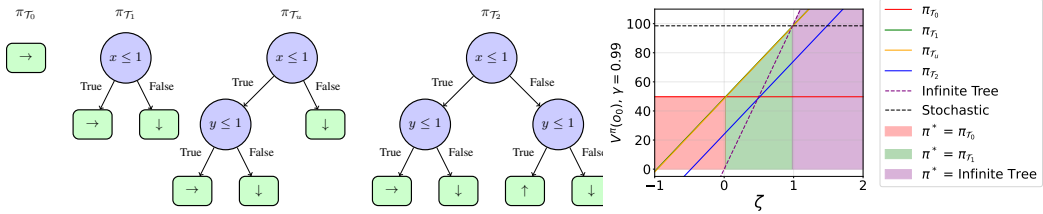


Figure 2: Decision tree policies and their RL objective values (definition 2) as functions of the rewards ζ in POIBMDPs associated to the grid world MDP (figure 1b). Shaded areas on the right plot indicate which deterministic memoryless policy is optimal depending on ζ . Recall that ζ can be seen as a reward that encourages the deterministic memoryless policy to take information-gathering actions, i.e. the reward that trades off interpretability of the corresponding decision tree and its cumulative reward.

312 depth-1 and unbalanced depth-2 tree, we now know from the green shaded area that a depth-1 tree
 313 is optimal when $0 < \zeta < 1$ in the POIBMDP. Interestingly, two challenges of learning in POMDPs
 314 described in Singh et al. (1994) are visible in figure 2. First, there is a whole range of ζ values for
 315 which the optimal memoryless policy is stochastic. Second, for e.g. $\zeta = 0.5$, while the optimal
 316 deterministic memoryless policy corresponds to a depth-1 tree, the value of the (PO)IBMDP state
 317 $(s_2, o_0) = (1.5, 1.5, 0, 2, 0, 2)$, i.e. the agent current position is upper right cell in the downstream
 318 MDP but it has not information about it, is not maximized by the optimal memoryless policy that
 319 will take 1 information-gathering action in between each downstream action (figure 2), but by the
 320 sub-optimal policy that always goes down. Next, we present the specific experimental setup that we
 321 use in the remaining of the paper.

322 5.2 Experimental setup

323 All our code is open source¹. The downstream MDP for which we want to learn decision tree
 324 policies with reinforcement learning is the grid world MDP (figure 1a). We then get 100 associated
 325 POIBMDPs following figure 1b with ζ chosen uniformly among 100 different in $]0, 1[$.

326 We will evaluate two types of reinforcement learning algorithm. First we use standard tabular RL
 327 algorithms, namely Q-learning, Sarsa, and vanilla policy gradient on a softmax policy Watkins &
 328 Dayan (1992); Sutton & Barto (1998); Jaakkola et al. (1994), to learn deterministic memoryless
 329 policies in POIBMDPs by simply replacing the current state in the algorithm descriptions by the
 330 current observation. In theory the policy gradient algorithm should not be a good candidate for
 331 our problem since it searches for stochastic policies that we showed can be better than our sought
 332 depth-1 decision tree policy (figure 2), but for completeness we will see what trees are obtained after
 333 greddification of the stochastic policies.

334 Second, we also use the more specialised asymmetric Q-learning, asymmetric Sarsa, and asymmetric
 335 policy gradient (algorithm 4, section 4.2). Each algorithm is trained until convergence on each
 336 POIBMDP, and each one of those runs is repeated 100 times. For all baselines we use, when applicable,
 337 exploration rates $\epsilon = 0.3$ and learning rates $\alpha = 0.1$. All the training curves are presented in
 338 appendix 11.

339 We will consider two metrics. We consider the distribution of the learned trees over the 100 training
 340 seeds. Indeed, since for every POIBMDP we run each algorithm 100 times, at the end of training we
 341 get 100 deterministic memoryless policies, from which we can extract the equivalent 100 decision
 342 tree policies using algorithm 1 and we can count which one have e.g. a depth of 1. This helps
 343 understand which trees RL algorithms tend to learn as a function of the trade-off reward ζ .

¹<https://anonymous.4open.science/r/poibmdps-5BFE/>

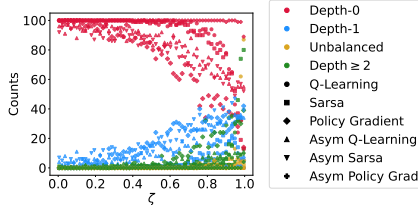


Figure 3: Distributions of final tree policies learned across the 100 seeds. For each ζ value, there are four colored points. Each point represent the share of depth-0 trees (red), depth-1 trees (green), unbalanced depth-2 trees (orange) and depth-2 trees (blue).

344 **5.3 Can reinforcement learning find the optimal deterministic memoryless POIBMDP
345 policies?**

346 In figure 13, we plot the distributions of the final learned trees over the 100 random seeds in function
347 of ζ from the above runs. For example, in figure 13, in the top left plot, when learning 100 times in
348 a POIBMDP with $\zeta = 0.5$, Q-learning returned almost 100 times a depth-0 tree. Again, on none of
349 those subplots do we see a high rate of learned depth-1 trees for $\zeta \in]0, 1[$. It is alerting that the most
350 frequent learned trees are the depth-0 trees for $\zeta \in]0, 1[$ because such trees are way more sub-optimal
351 than e.g. the depth-2 unbalanced trees (figure 2). One interpretation of this phenomenon is that the
352 learning in POIBMDPs is very difficult and so agents tend to converge to trivial policies, e.g., repeating
353 the same downstream action. Furhtermore, in appendix 11 we show that for POIBMDPs with
354 $\zeta \in [-1, 0]$ and $\zeta \in [1, 2]$, baselines consistently learn the optimal policies—a depth-0 tree and an
355 infinite tree respectively—which is concerning as it means that RL seem to find only trivial policies.
356 On the positive side, we observe that asymmetric versions of Q-learning and Sarsa have found the
357 optimal deterministic memoryless policy—the depth-1 decision tree—more frequently throughout the
358 optimality range $]0, 1[$, than their symmetric counter-parts for $\zeta \in]0, 1[$. Next, we quantify how difficult
359 it is to do RL to learn memoryless policies in POIBMDPs as opposed to standard Markovian
360 polcicies.

361 **5.4 How difficult is it to learn in POIBMDPs?**

362 In this section we run the same (asymmetric) reinforcement learning algorithms to learn standard
363 Markovian policies in MDPs (definition 1) or IBMDPs (definition 5), or deterministic memoryless
364 policies in POIBMDPs (definition 7).

365 In order to see how difficult each of these three problems is, we can run a *great* number of ex-
366 periments for each problem and compare solving rates. To make solving rates comparable we
367 consider a unique instance for each of those problems. Problem 1 is learning one of the optimal
368 standard Markovian deterministic policy ($\pi : S \rightarrow A$)from figure 1a for the grid world MDP
369 with $\gamma = 0.99$. Problem 2 is learning one of the optimal standard Markovian deterministic policy
370 ($\pi : S \times O \rightarrow A \cup A_{info}$) for the IBMDP from figure 1b with $\gamma = 0.99$ and $\zeta = 0.5$. Prob-
371 lem 3 is what has been done in the previous section to learn deterministic memoryless policies
372 ($\pi : O \rightarrow A \cup A_{info}$) where in addition of fixing $\gamma = 0.99$ we also fix $\zeta = 0.5$.

373 We use the six (asymmetric) RL algorithms from the previous section and try a wide set of hy-
374 perparameters and additional learning tricks (optimistic Q-function, eligibility traces, entropy reg-
375 ularization and ϵ -decay, all are described in Sutton & Barto (1998)). The complete detailed lists
376 of hyperparameters are given in the appendix 12 and a summary is given in table 6. Furthermore,
377 the careful reader might notice that there is no point running asymmetric RL on MDPs or IBMDPs
378 when the problem does not require partial observability. Hence, we only run asymmetric RL for
379 POIBMDPs and otherwise run all other RL algorithms and all problems.

380 Each unique hyperparameter combination for a given algorithm on a given problem is run 10 times
381 on 1 million learning steps to get standard errors. For example, for asymmetric Sarsa, we run a total

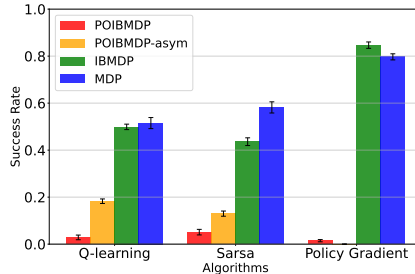


Figure 4: Success rates of different (asymmetric) RL algorithms over thousands of runs when applied to learning deterministic memoryless policies in a POIBMDP or learning deterministic policies in associated MDP and IBMDP.

382 of $10 \times 768 = 7680$ experiments for learning deterministic memoryless policies for a POIBMDP. To
 383 get a success rate, we can simply divide the number of learned optimal depth-1 tree by 768 (recall
 384 that for $\gamma = 0.99$ and $\zeta = 0.5$, the optimal policy is a depth-1 tree (e.g. figure 2)).

385 The key observations from figure 4 is that reinforcement learning a deterministic memoryless policy
 386 in a POIBMDP, is way harder than learning a standard Markovian policy. For example, Q-learning
 387 finds the optimal solution in only 3% of the experiments while the same algorithms to optimize the
 388 standard RL objective (definition 2) in an MDP or IBMDP found the optimal solutions 50% of the
 389 time. Even though asymmetry seems to increase performances; learning a decision tree policy for a
 390 simple grid world directly with RL using the framework of POIBMDP originally developed in Topin
 391 et al. (2021) seems way too difficult and costly as successes might require a million steps for such a
 392 seemingly simple problem. An other difficulty in practice that we did not cover here, is the choice
 393 of information gathering actions. For the grid world MDP, choosing good IGAs ($x \leq 1$ and $y \leq 1$)
 394 is simple but what about more complicated MDPs: how to instantiate the (PO)IBMDP action space
 395 such that internal nodes in resulting trees are useful for predictions? Next, we further support that
 396 partial observability is the main limitation for reinforcement learning to train decision tree policies
 397 for MDPs.

398 5.5 Are they downstream MDPs for which partial observability is not a limitation?

399 In this section, we show that for a special class of POIBMDPs, reinforcement learning can learn
 400 optimal deterministic memoryless policies w.r.t the RL objective, i.e. we can do direct decision
 401 tree policy learning for MDPs. This class of POIBMDPs are those for which downstream MDPs
 402 have uniform transitions, i.e. $T(s, a, s') = \frac{1}{|S'|}$ (definitions 1 and 5). Such downstream MDPs in-
 403 clude classification tasks formulated as MDPs. This implies that learning deterministic memoryless
 404 policies in POIBMDPs where the downstream MDP encodes a classification task is equivalent to
 405 doing supervised learning of a decision tree (figure 5). This is exactly what is done in e.g. Kohler
 406 et al. (2025a). In figure 5 we give an example of such downstream MDPs for a classification task
 407 with 4 data in the training set and 2 classes: $\mathcal{X} = \{(0.5, 0.5), (0.5, 1.5), (1.5, 1.5), (1.5, 0.5)\}$ and
 408 $y = \{0, 0, 1, 1\}$.

409 In appendix 13, we show that POIBMDPs associated to downstream MDPs with uniform transitions
 410 are themselves standard MDP (definition 1). This means that in principle, standard RL algorithms
 411 like Q-learning, should work as well as for any MDP. If RL does work for such fully observable
 412 POIBMDPs, this would mean that the difficulty of direct learning of decision tree policies for *any*
 413 MDP using POIBMDPs, exhibited in sections, is most likely due to the partial observability. This
 414 is exactly what we check next. We use the same direct approach to learn decision tree policies as in
 415 previous sections, except that now the downstream MDP is a classification task and not a sequential
 416 decision making task like reaching a goal in a grid world.

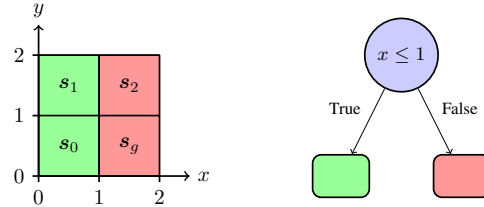


Figure 5: In this MDP, there are four data to which to assign either a green or red label. On the right, there is the unique optimal depth-1 tree for this particular MDP. This depth-1 tree also maximizes the accuracy on the corresponding classification task.

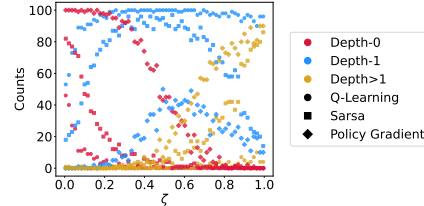


Figure 6: We reproduce the same plot as in figure 13 for POIBMDPs associated to a downstream MDP encoding a classification task. Each colored dot is the number of final learned trees with a specific structure for a given ζ .

417 We construct POIBMDPs for the classification task from figure 5, with $\gamma = 0.99$, 200 values of
 418 $\zeta \in [0, 1]$ and IGAs $x \leq 1$ and $y \leq 1$. Since those POIBMDPs are MDPs, we do not need to
 419 analyze asymmetric RL baselines. We see on figure 6 that compared to general POIBMDPs from
 420 previous sections, RL can be used to consistently learn optimal deterministic memoryless policies
 421 $O : \rightarrow A \cup A_{info}$. Such policies are equivalent to decision tree classifiers.

422 6 Discussion

423 In this paper, we were interested in algorithms that can learn decision tree policies that directly op-
 424 timize some trade-off of interpretability and performance in MDPs without relying on an oracle or
 425 expert policy. Starting from the IBMMDP formulation from Topin et al. (2021), we have shown that
 426 direct learning of decision tree policies for MDPs can be framed as learning deterministic mem-
 427 oryless policies in POMDPs that we called POIBMDPs. By bridging the gap with the POMDP
 428 literature, we conjectured that partial observability is the main limitation for reinforcement learning
 429 of decision tree policies for MDPs. We then supported this conjecture by benchmarking different
 430 reinforcement learning algorithms on carefully crafted problems for which we knew the exact opti-
 431 mal decision tree policies. Across our experiments, we found that only when partial observability is
 432 absent from the learning task can good decision tree policies be trained. Attempting to overcome the
 433 partial observability challenges highlighted so far seems like a bad research direction. Indeed, while
 434 algorithms tailored specifically for the problem of learning deterministic memoryless policies for
 435 POIBMDPs might exist, imitation learning works well in practice and has been the state-of-the-art
 436 for interpretable sequential decision making for a while. Furthermore there are other limitations that
 437 we did not cover in the framework of Topin et al. (2021) such as how to choose good candidates
 438 information-gathering actions or simply how to choose ζ for a target interpretability-performance
 439 trade-off. Finally, while we focused on non-parametric tree learning assuming RL algorithms should
 440 naturally trade off interpretability and performance through the reward signal ζ for adding nodes to
 441 the decision tree policy, another future research avenue could be to develop better algorithms training
 442 parametric trees. Indeed parametric tree policies, on the other hand, can be computed with
 443 reinforcement learning directly in the downstream MDP. However such RL algorithms for paramet-
 444 ric decision tree policies Silva et al. (2020); Vos & Verwer (2024); Marton et al. (2025) require to

445 re-train a policy entirely for each desired level of interpretability, i.e. each unique tree structure. Future
446 research in this direction should focus on algorithms for parametric tree policies that can re-use
447 samples from one tree learning to train a different tree structure more efficiently. This would reduce
448 the required quantity of a priori knowledge on the decision tree policy structure.

449 **Broader Impact Statement**

450 Our work put great emphasis on covering existing work, open sourcing code, and being transparent
451 about limitations. We hope that the impact of our work is going to be positive for society through
452 advancing research in interpretable machine learning.

453 **Acknowledgments**

454 Use unnumbered third level headings for the acknowledgments. All acknowledgments, including
455 those to funding agencies, go at the end of the paper. Only add this information once your submission
456 is accepted and deanonymized. The acknowledgments do not count towards the 8–12 page limit.

457 **References**

- 458 Mauricio Araya-López, Vincent Thomas, Olivier Buffet, and François Charpillet. A Closer Look
459 at MOMDPs. In *Proceedings of the 22nd International Conference on Tools with Artificial*
460 *Intelligence*, Proceedings of the 22nd International Conference on Tools with Artificial In-
461 telligence, Arras, France, October 2010. IEEE. URL [https://inria.hal.science/
462 inria-00535559](https://inria.hal.science/inria-00535559).
- 463 Akanksha Atrey, Kaleigh Clary, and David Jensen. Exploratory not explanatory: Counterfactual
464 analysis of saliency maps for deep reinforcement learning. In *International Conference on Learn-
465 ing Representations*, 2020. URL <https://openreview.net/forum?id=rkl3m1BFDB>.
- 466 Andrea Baisero and Christopher Amato. Unbiased asymmetric reinforcement learning under partial
467 observability. In *Proceedings of the 21st International Conference on Autonomous Agents and*
468 *Multiagent Systems*, AAMAS ’22, pp. 44–52, Richland, SC, 2022. International Foundation for
469 Autonomous Agents and Multiagent Systems. ISBN 9781450392136.
- 470 Andrea Baisero, Brett Daley, and Christopher Amato. Asymmetric DQN for partially observ-
471 able reinforcement learning. In James Cussens and Kun Zhang (eds.), *Proceedings of the*
472 *Thirty-Eighth Conference on Uncertainty in Artificial Intelligence*, volume 180 of *Proceed-
473 ings of Machine Learning Research*, pp. 107–117. PMLR, 01–05 Aug 2022. URL <https://proceedings.mlr.press/v180/baisero22a.html>.
- 475 Andrew G. Barto, Richard S. Sutton, and Charles W. Anderson. Neuronlike adaptive elements
476 that can solve difficult learning control problems. *IEEE Transactions on Systems, Man, and*
477 *Cybernetics*, SMC-13(5):834–846, 1983. DOI: 10.1109/TSMC.1983.6313077.
- 478 Osbert Bastani, Yewen Pu, and Armando Solar-Lezama. Verifiable reinforcement learning via policy
479 extraction. 2018.
- 480 Richard Bellman. *Dynamic Programming*. 1957.
- 481 Dimitris Bertsimas and Jack Dunn. Optimal classification trees. *Machine Learning*, 106:1039–1082,
482 2017.
- 483 Guy Blanc, Jane Lange, and Li-Yang Tan. Learning stochastic decision trees. *CoRR*,
484 abs/2105.03594, 2021. URL <https://arxiv.org/abs/2105.03594>.
- 485 L Breiman, JH Friedman, R Olshen, and CJ Stone. *Classification and Regression Trees*. Wadsworth,
486 1984.

- 487 Samuel Ping-Man Choi, Nevin Lianwen Zhang, and Dit-Yan Yeung. Solving hidden-mode markov
488 decision problems. In Thomas S. Richardson and Tommi S. Jaakkola (eds.), *Proceedings of*
489 *the Eighth International Workshop on Artificial Intelligence and Statistics*, volume R3 of *Pro-*
490 *ceedings of Machine Learning Research*, pp. 49–56. PMLR, 04–07 Jan 2001. URL <https://proceedings.mlr.press/r3/choi01a.html>. Reissued by PMLR on 31 March
492 2021.
- 493 Emir Demirovic, Anna Lukina, Emmanuel Hebrard, Jeffrey Chan, James Bailey, Christopher
494 Leckie, Kotagiri Ramamohanarao, and Peter J. Stuckey. Murtree: Optimal decision trees via
495 dynamic programming and search. *Journal of Machine Learning Research*, 23(26):1–47, 2022.
496 URL <http://jmlr.org/papers/v23/20-520.html>.
- 497 Emir Demirović, Emmanuel Hebrard, and Louis Jean. Blossom: an anytime algorithm for com-
498 puting optimal decision trees. *Proceedings of the 40th International Conference on Machine*
499 *Learning*, 202:7533–7562, 23–29 Jul 2023. URL <https://proceedings.mlr.press/v202/demirovic23a.html>.
- 501 Claire Glanois, Paul Weng, Matthieu Zimmer, Dong Li, Tianpei Yang, Jianye Hao, and Wulong Liu.
502 A survey on interpretable reinforcement learning. *Machine Learning*, pp. 1–44, 2024.
- 503 Tommi Jaakkola, Satinder P. Singh, and Michael I. Jordan. Reinforcement learning algorithm for
504 partially observable markov decision problems. In *Proceedings of the 8th International Confer-*
505 *ence on Neural Information Processing Systems*, NIPS’94, pp. 345–352, Cambridge, MA, USA,
506 1994. MIT Press.
- 507 Hector Kohler, Riad Akour, and Philippe Preux. Breiman meets bellman: Non-greedy decision
508 trees with mdps. In *Proceedings of the 31st ACM SIGKDD Conference on Knowledge Discovery*
509 *and Data Mining V.2*, KDD ’25, pp. 1207–1218, New York, NY, USA, 2025a. Association for
510 Computing Machinery. ISBN 9798400714542. DOI: 10.1145/3711896.3736868. URL <https://doi.org/10.1145/3711896.3736868>.
- 512 Hector Kohler, Waris Radji, Quentin Delfosse, Riad Akour, and Philippe Preux. Evaluating inter-
513 pretable reinforcement learning by distilling policies into programs. In *RLC 2025 Workshop on*
514 *Programmatic Reinforcement Learning*, 2025b. URL <https://openreview.net/forum?id=n1CfzixauT>.
- 516 Gaspard Lambrechts, Adrien Bolland, and Damien Ernst. Informed POMDP: Leveraging additional
517 information in model-based RL. *Reinforcement Learning Journal*, 2:763–784, 2025a.
- 518 Gaspard Lambrechts, Damien Ernst, and Aditya Mahajan. A theoretical justification for asymmetric
519 actor-critic algorithms. In *Forty-second International Conference on Machine Learning*, 2025b.
520 URL <https://openreview.net/forum?id=FlyANMCnAn>.
- 521 Zachary C. Lipton. The mythos of model interpretability: In machine learning, the concept of
522 interpretability is both important and slippery. *Queue*, 16(3):31–57, 2018.
- 523 Michael L. Littman. Memoryless policies: theoretical limitations and practical results. In *Proceed-*
524 *ings of the Third International Conference on Simulation of Adaptive Behavior: From Animals to*
525 *Animats 3: From Animals to Animats 3*, SAB94, pp. 238–245, Cambridge, MA, USA, 1994. MIT
526 Press. ISBN 0262531224.
- 527 John Loch and Satinder P. Singh. Using eligibility traces to find the best memoryless policy in
528 partially observable markov decision processes. In *Proceedings of the Fifteenth International*
529 *Conference on Machine Learning*, ICML ’98, pp. 323–331, San Francisco, CA, USA, 1998.
530 Morgan Kaufmann Publishers Inc. ISBN 1558605568.
- 531 Scott M. Lundberg and Su-In Lee. A unified approach to interpreting model predictions. In *Proceed-*
532 *ings of the 31st International Conference on Neural Information Processing Systems*, NIPS’17,
533 pp. 4768–4777, Red Hook, NY, USA, 2017. Curran Associates Inc. ISBN 9781510860964.

- 534 Yishay Mansour, Michal Moshkovitz, and Cynthia Rudin. There is no accuracy-interpretability
535 tradeoff in reinforcement learning for mazes, 2022. URL <https://arxiv.org/abs/2206.04266>.
- 537 Sascha Marton, Tim Grams, Florian Vogt, Stefan Lüdtke, Christian Bartelt, and Heiner Stucken-
538 schmidt. Mitigating information loss in tree-based reinforcement learning via direct optimization.
539 2025. URL <https://openreview.net/forum?id=qpXctF2aLZ>.
- 540 Stephanie Milani, Nicholay Topin, Manuela Veloso, and Fei Fang. Explainable reinforcement learn-
541 ing: A survey and comparative review. *ACM Comput. Surv.*, 56(7), April 2024. ISSN 0360-0300.
542 DOI: 10.1145/3616864. URL <https://doi.org/10.1145/3616864>.
- 543 Volodymyr Mnih, Koray Kavukcuoglu, David Silver, Andrei A Rusu, Joel Veness, Marc G Belle-
544 mare, Alex Graves, Martin Riedmiller, Andreas K Fidjeland, Georg Ostrovski, et al. Human-level
545 control through deep reinforcement learning. *nature*, 518(7540):529–533, 2015.
- 546 Sreerama Murthy and Steven Salzberg. Lookahead and pathology in decision tree induction. In
547 *Proceedings of the 14th International Joint Conference on Artificial Intelligence - Volume 2*,
548 IJCAI’95, pp. 1025–1031, San Francisco, CA, USA, 1995. Morgan Kaufmann Publishers Inc.
549 ISBN 1558603638.
- 550 F. Pedregosa, G. Varoquaux, A. Gramfort, V. Michel, B. Thirion, O. Grisel, M. Blondel, P. Pretten-
551 hofer, R. Weiss, V. Dubourg, J. Vanderplas, A. Passos, D. Cournapeau, M. Brucher, M. Perrot, and
552 E. Duchesnay. Scikit-learn: Machine learning in Python. *Journal of Machine Learning Research*,
553 12:2825–2830, 2011.
- 554 Lerrel Pinto, Marcin Andrychowicz, Peter Welinder, Wojciech Zaremba, and Pieter Abbeel. Asym-
555 metric actor critic for image-based robot learning, 2017. URL <https://arxiv.org/abs/1710.06542>.
- 557 Nikaash Puri, Sukriti Verma, Piyush Gupta, Dhruv Kayastha, Shripad Deshmukh, Balaji Krishnamurthy,
558 and Sameer Singh. Explain your move: Understanding agent actions using specific and relevant feature
559 attribution. In *International Conference on Learning Representations*, 2020. URL
560 <https://openreview.net/forum?id=SJgzIkBKPB>.
- 561 Antonin Raffin, Ashley Hill, Adam Gleave, Anssi Kanervisto, Maximilian Ernestus, and Noah Dor-
562 man. Stable-baselines3: Reliable reinforcement learning implementations. *Journal of Machine
563 Learning Research*, 22(268):1–8, 2021.
- 564 Marco Tulio Ribeiro, Sameer Singh, and Carlos Guestrin. "why should i trust you?": Explaining
565 the predictions of any classifier. pp. 1135–1144, 2016. DOI: 10.1145/2939672.2939778. URL
566 <https://doi.org/10.1145/2939672.2939778>.
- 567 Stéphane Ross, Geoffrey J. Gordon, and J. Andrew Bagnell. A reduction of imitation learning and
568 structured prediction to no-regret online learning. 2010.
- 569 John Schulman, Filip Wolski, Prafulla Dhariwal, Alec Radford, and Oleg Klimov. Proximal policy
570 optimization algorithms. *arXiv preprint arXiv:1707.06347*, 2017.
- 571 Wenjie Shi, Gao Huang, Shiji Song, Zhuoyuan Wang, Tingyu Lin, and Cheng Wu. Self-supervised
572 discovering of interpretable features for reinforcement learning. *IEEE Transactions on Pat-
573 tern Analysis and Machine Intelligence*, 44(5):2712–2724, 2022. DOI: 10.1109/TPAMI.2020.
574 3037898.
- 575 Olivier Sigaud and Olivier Buffet. *Partially Observable Markov Decision Processes*, chapter 7,
576 pp. 185–228. John Wiley Sons, Ltd, 2013. ISBN 9781118557426. DOI: <https://doi.org/10.1002/9781118557426.ch7>. URL <https://onlinelibrary.wiley.com/doi/abs/10.1002/9781118557426.ch7>.

- 579 Andrew Silva, Matthew Gombolay, Taylor Killian, Ivan Jimenez, and Sung-Hyun Son. Optimization
580 methods for interpretable differentiable decision trees applied to reinforcement learning. In
581 Silvia Chiappa and Roberto Calandra (eds.), *Proceedings of the Twenty Third International Conference*
582 on Artificial Intelligence and Statistics
- 583 , volume 108 of *Proceedings of Machine Learning Research*, pp. 1855–1865. PMLR, 26–28 Aug 2020. URL <https://proceedings.mlr.press/v108/silva20a.html>.
- 585 Satinder P. Singh, Tommi S. Jaakkola, and Michael I. Jordan. Learning without state-estimation
586 in partially observable markovian decision processes. In *Proceedings of the Eleventh Interna-*
587 *tional Conference on International Conference on Machine Learning*, ICML’94, pp. 284–292,
588 San Francisco, CA, USA, 1994. Morgan Kaufmann Publishers Inc. ISBN 1558603352.
- 589 Edward J. Sondik. The optimal control of partially observable markov processes over the infi-
590 nite horizon: Discounted costs. *Operations Research*, 26(2):282–304, 1978. ISSN 0030364X,
591 15265463. URL <http://www.jstor.org/stable/169635>.
- 592 Richard S. Sutton and Andrew G. Barto. *Reinforcement Learning: An Introduction*. The MIT Press,
593 Cambridge, MA, 1998.
- 594 Richard S Sutton, David McAllester, Satinder Singh, and Yishay Mansour. Policy gradient
595 methods for reinforcement learning with function approximation. In S. Solla, T. Leen, and
596 K. Müller (eds.), *Advances in Neural Information Processing Systems*, volume 12. MIT Press,
597 1999. URL https://proceedings.neurips.cc/paper_files/paper/1999/file/464d828b85b0bed98e80ade0a5c43b0f-Paper.pdf.
- 599 Nicholay Topin, Stephanie Milani, Fei Fang, and Manuela Veloso. Iterative bounding mdps: Learn-
600 ing interpretable policies via non-interpretable methods. *Proceedings of the AAAI Conference on*
601 *Artificial Intelligence*, 35:9923–9931, 2021.
- 602 Mark Towers, Ariel Kwiatkowski, Jordan Terry, John U Balis, Gianluca De Cola, Tristan Deleu,
603 Manuel Goulão, Andreas Kallinteris, Markus Krimmel, Arjun KG, et al. Gymnasium: A standard
604 interface for reinforcement learning environments. *arXiv preprint arXiv:2407.17032*, 2024.
- 605 Jacobus van der Linden, Mathijs de Weerdt, and Emir Demirović. Necessary and sufficient condi-
606 tions for optimal decision trees using dynamic programming. *Advances in Neural Information*
607 *Processing Systems*, 36:9173–9212, 2023.
- 608 Abhinav Verma, Vijayaraghavan Murali, Rishabh Singh, Pushmeet Kohli, and Swarat Chaudhuri.
609 Programmatically interpretable reinforcement learning. pp. 5045–5054, 2018.
- 610 Sicco Verwer and Yingqian Zhang. Learning optimal classification trees using a binary linear pro-
611 gram formulation. *Proceedings of the AAAI conference on artificial intelligence*, 33:1625–1632,
612 2019.
- 613 Daniël Vos and Sicco Verwer. Optimal decision tree policies for markov decision processes. In
614 *Proceedings of the Thirty-Second International Joint Conference on Artificial Intelligence*, IJCAI
615 ’23, 2023. ISBN 978-1-956792-03-4. DOI: 10.24963/ijcai.2023/606. URL <https://doi.org/10.24963/ijcai.2023/606>.
- 617 Daniël Vos and Sicco Verwer. Optimizing interpretable decision tree policies for reinforcement
618 learning. 2024. URL <https://arxiv.org/abs/2408.11632>.
- 619 Christopher JCH Watkins and Peter Dayan. Q-learning. *Machine learning*, 8(3):279–292, 1992.
- 620 Haoze Wu, Omri Isac, Aleksandar Zeljić, Teruhiro Tagomori, Matthew Daggitt, Wen Kokke, Idan
621 Refaeli, Guy Amir, Kyle Julian, Shahaf Bassan, Pei Huang, Ori Lahav, Min Wu, Min Zhang, Eka-
622 terina Komendantskaya, Guy Katz, and Clark Barrett. Marabou 2.0: A versatile formal analyzer
623 of neural networks, 2024. URL <https://arxiv.org/abs/2401.14461>.

Data: Deterministic partially observable policy π_{po} for IBMDP
 $\mathcal{M}_{IB} \equiv \langle S \times O, A \cup A_{info}, (R, \zeta), (T_{info}, T, T_0) \rangle$ and IBMDP observation
 $\mathbf{o} = (L'_1, U'_1, \dots, L'_p, U'_p)$

Result: Decision tree policy π_T for MDP $\mathcal{M} \equiv \langle S, A, R, T, T_0 \rangle$

Function Subtree_From_Policy(\mathbf{o}, π_{po}):

```
a ← πpo(o)
if a is a downstream action then
|   return Leaf_Node(action: a)
end
else
|   ⟨i, v⟩ ← a
|   oL ← o; oR ← o
|   oL ← (L'_1, U'_1, ..., L'_j, v, ..., L'_p, U'_p); oR ← (L'_1, U'_1, ..., v, U'_j, ..., L'_p, U'_p)
|   childL ← Subtree_From_Policy(oL, πpo)
|   childR ← Subtree_From_Policy(oR, πpo)
|   return Internal_Node(feature: i, value: v, children: (childL, childR))
end
```

Algorithm 1: Extract a decision tree policy (algorithm 1 from [Topin et al. \(2021\)](#))

624
625
626

Supplementary Materials

The following content was not necessarily subject to peer review.

627

7 From a policy to a tree

628

8 Imitation learning: a baseline for indirect decision tree policy learning

629
630
631
632
633
634
635
636
637

In this section we present decision tree policies of this manuscript obtained using Dagger or VIPER [Bastani et al. \(2018\)](#); [Verma et al. \(2018\)](#) after learning an expert Q-function for the grid world MDP. Recall the optimal policies for the grid world, taking the green actions in each state in figure 1a. Among the optimal policies, the ones that go left or up in the goal state can be problematic for imitation learning algorithms. Indeed, we know that for this grid world MDP there exists decision tree policies with a very good interpretability-performance trade-off: depth-1 decision trees that are optimal w.r.t. the RL objective. One could even say that those trees have the *optimal* interpretability-performance trade-off because they are the shortest trees that are optimal w.r.t. the RL objective.

638
639
640

In figure 7, we present a depth-1 decision tree policy that is optimal w.r.t. the RL objective and a depth-1 tree that is sub-optimal. The other optimal depth-1 tree is to go right when $y \leq 1$ and down otherwise.

641
642

Now a fair question is: can Dagger or VIPER learn such an optimal depth-1 tree given access to an expert optimal policy from figure 1a?

643
644
645
646
647
648
649

We start by running the standard Q-learning algorithm with $\epsilon = 0.3$, $\alpha = 0.1$ over 10,000 time steps. While for Q-learning, Sutton and Barto break ties by index value in their book [Sutton & Barto \(1998\)](#) (the greedy action is the argmax action with smallest index), we show that the choice of tie-breaking greatly influences the performance of subsequent imitation learning algorithms. Indeed, depending on how actions are ordered in practice, Q-learning may be biased toward some optimal policies rather than others. While this does not matter for one who just wants to find an optimal policy, in our example of finding the optimal depth-1 decision tree policy, it matters *a lot*.

650
651
652

In the left plot of figure 8, we see that Q-learning, independently of how ties are broken, consistently converges to an optimal policy over 100 runs (random seeds). However, in the right plot of figure 8, where we plot the proportion over 100 runs of optimal decision trees returned by Dagger or VIPER

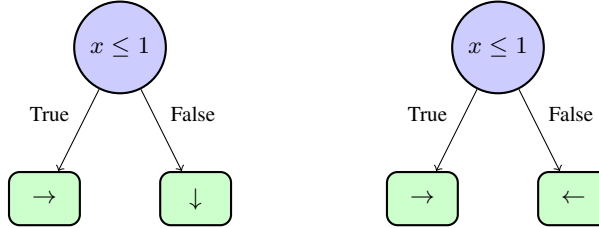


Figure 7: Left, an optimal depth-1 decision tree policy for the grid world MDP from figure 1a. On the right, a sub-optimal depth-1 decision tree policy.

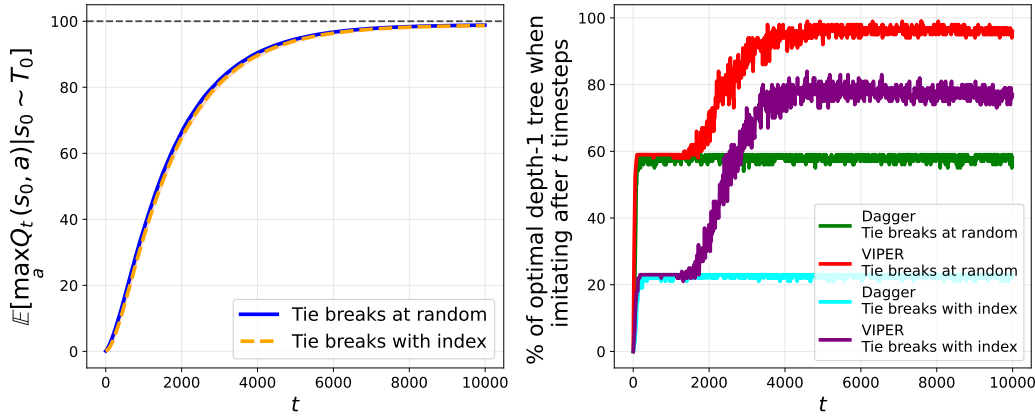


Figure 8: Left, sample complexity curve of Q-learning with default hyperparameters on the 2×2 grid world MDP over 100 random seeds. Right, performance of indirect interpretable methods when imitating the greedy policy with a tree at different Q-learning stages.

at different stages of Q-learning, we observe that imitating the optimal policy obtained by breaking ties at random consistently yields more optimal trees than breaking ties by indices. What actually happens is that the most likely output of Q-learning when ties are broken by indices is the optimal policy that goes left in the goal state, which cannot be perfectly represented by a depth-1 decision tree, because there are three different actions taken and a binary tree of depth $D = 1$ can only map to $2^D = 2$ labels.

This short experiment shows that imitation learning approaches can sometimes be very bad at learning decision tree policies with good interpretability-performance trade-offs for very simple MDPs. Despite VIPER almost always finding the optimal depth-1 decision tree policy in terms of the RL objective when ties are broken at random, we have shed light on the sub-optimality of indirect approaches such as imitation learning. This motivates the study of direct approaches to directly search for policies with good interpretability-performance trade-offs with respect to the original RL objective.

9 Reproducing “Iterative Bounding MDPs: Learning Interpretable Policies via Non-Interpretable Methods”

We attempt to reproduce the results from Topin et al. (2021) in which authors compare direct and indirect learning of decision tree policies of depth at most 2 for the CartPole MDP Barto et al. (1983). In the original paper, the authors find that both direct and indirect learning yields decision tree policies with similar RL objective values (definition 2) for the CartPole. On the other hand, we find that, imitation learning, despite not directly optimizing the RL objective for CartPole, outperforms deep RL which directly optimizes a trade-off of the standard RL objective and interpretability.

674 Authors of [Topin et al. \(2021\)](#) use two deep reinforcement learning baselines to which they apply
675 some modifications in order to learn memoryless policies. Authors modify the standard DQN ? to
676 return a memoryless policy. The trained Q -function is approximated with a neural network $O \rightarrow \mathbb{R}^{|A \cup A_{info}|}$ rather than $S \times O \rightarrow \mathbb{R}^{|A \cup A_{info}|}$. In this modified DQN, the temporal difference error
677 target for the Q -function $O \rightarrow A \cup A_{info}$ is approximated by a neural network $S \times O \rightarrow A \cup A_{info}$
678 that is in turn trained by bootstrapping the temporal difference error with itself. We present the
679 modifications in algorithm 2. Similar modifications are applied to the standard PPO [Schulman et al.](#)
680 ([2017](#)) that we present in the appendix (algorithm 3). In the modified PPO, neural network policy
681 $O \rightarrow A \cup A_{info}$ is trained using a neural network value function $S \times O \rightarrow A \cup A_{info}$ as a critic.
682

683 Those two variants of DQN and PPO have first been introduced in [Pinto et al. \(2017\)](#) for robotic tasks
684 with partially observable components, under the name “asymmetric” actor-critic. Asymmetric RL
685 algorithms that have policy and value estimates using different information from a POMDP [Sondik](#)
686 ([1978](#)); [Sigaud & Buffet \(2013\)](#) were later studied theoretically to solve POMDPs in Baisero’s
687 work [Baisero et al. \(2022\)](#); [Baisero & Amato \(2022\)](#). The connections from Deep RL in IBMDPs
688 for objective is absent from [Topin et al. \(2021\)](#) and we defer their connections to direct interpretable
689 reinforcement learning to the next chapter as our primary goal is to reproduce [Topin et al. \(2021\) as is](#).
690 Next, we present the precise experimental setup we use to reproduce [Topin et al. \(2021\)](#) in order
691 to study direct deep reinforcement learning of decision tree policies for the CartPole MDP.

692 9.1 IBMDP formulation

693 Given a base MDP $\mathcal{M} \equiv \langle S, A, R, T, T_0 \rangle$ (cf. definition 1), in order to define an IBMDP
694 $\mathcal{M}_{IB} \langle S \times O, A \cup A_{info}, (R, \zeta), (T, T_0, T_{info}) \rangle$ (cf. definition 5), the user needs to provide the
695 set of information gathering actions A_{info} and the reward ζ for taking those. Authors of [Topin](#)
696 [et al. \(2021\)](#) propose to parametrize the set of IGAs with $j \times q$ actions $\langle j, v_k \rangle$ with v_k depending
697 on the current observation $\mathbf{o}_t = (L'_1, U'_1, \dots, L'_j, U'_j, \dots, L'_p, U'_p)$: $v_k = \frac{k(U'_j - L'_j)}{q+1}$. This parametric
698 IGAs space keeps the discrete IBMDP action space at a reasonable size while providing a learning
699 algorithm with varied IGAs to try.

700 For example, if we define an IBMDP with $q = 3$ for the grid world from figure 1a, the grid world
701 action space is augmented with six IGAs. At $t = 0$, recall that $\mathbf{o}_0 = (0, 2, 0, 2)$, so if an IGA is taken,
702 e.g. $\langle 2, v_2 \rangle$, the effective IGA is $\langle j, v_2 = \frac{k(2-0)}{3+1} \rangle = \langle 1, 2 \rangle$ which in turn effectively corresponds
703 to an internal decision tree node $y \leq 1$. If the current state y -feature value is 0.5, then the next
704 observation at $t = 1$ is $\mathbf{o}_1 = (0, 2, 0, 1)$. At $t = 2$ if $a_t = \langle 2, v_2 \rangle$ again, it would be effectively
705 $\langle j, v_2 = \frac{k(1-0)}{3+1} \rangle = \langle 2, 0.5 \rangle$. This would give the next observation at $t = 2$ $\mathbf{o}_2 = (0, 2, 0, 0.5)$ and
706 so on.

707 Furthermore, author propose to regularize the learned decision tree policy with a maximum depth
708 parameter D . Unfortunately, the authors did not describe how they implemented the depth control
709 in their work, hence we have to try different approaches to reproduce their results.

710 To control the tree depth during learning in the IBMDP, we can either give negative reward for taking
711 D IGAs in a row, or terminate the trajectory. In practice, we could also have a state-dependent action
712 space such that taking an IGA is not allowed after taking D IGAs in a row. The latter approach—
713 sometimes called action masking—is not compatible with the definition of an MDP (cf. definition 1)
714 in which all actions are available in all states. To apply the penalization approaches, one can extend
715 the MDP states to keep track of the current tree depth. Similarly, the termination approach requires
716 a transition function that depends on the current tree depth.

717 We actually find that when $q + 1$, the parameter that defines threshold values in decision tree policy
718 nodes (cf. definition 5), is a prime number, then as a direct consequence of the *Chinese Remainder*
719 *Theorem*², the current tree depth is directly encoded in the current observation \mathbf{o}_t . Hence, when
720 $q + 1$ is prime, we can control the depth through either transitions or rewards without tracking the

²https://en.wikipedia.org/wiki/Chinese_remainder_theorem

Table 1: IBMDP hyperparameters. We try 12 different IBMDPs. In green we highlight the hyperparameters from the original paper and in red we highlight the hyperparameter names for which author do not give information.

Hyperparameter	Values
Discount factor γ	1
Information gathering actions parameter q	2, 3
Information gathering actions rewards ζ	-0.01, 0.01
Depth control	Done signal, negative reward, none

Table 2: (Modified) DQN trained on 10^6 timesteps. This gives four different instantiation of (modified) DQN. Hyperparameters not mentioned are stable-baselines3 default. In green we highlight the hyperparameters from the original paper and in red we highlight the hyperparameter names for which author do not give information.

Hyperparameter	Values
Buffer size	10^6
Random transitions before learning	10^5
Epsilon start	0.9, 0.5
Epsilon end	0.05
Exploration fraction	0.1
Optimizer	RMSprop ($\alpha = 0.95$)
Learning rate	2.5×10^{-4}
Networks architectures	[128, 128]
Networks activations	tanh(), relu()

721 tree depth. We use the exact same downstream MDP and associated IBMDPs for our experiments
 722 as [Topin et al. \(2021\)](#) except when mentioned otherwise.

723 **downstream MDP** The task at hand is to optimize the RL objective (definition 2) with a decision
 724 tree policy for the CartPole MDP [Barto et al. \(1983\)](#). At each time step a learning algorithm observes
 725 the cart’s position and velocity and the pole’s angle and angular velocity, and can take action to push
 726 the CartPole left or right. While the CartPole is roughly balanced, i.e., while the cart’s angle remains
 727 in some fixed range, the agent gets a positive reward. If the CartPole is out of balance, the MDP
 728 transitions to an absorbing terminal state and gets 0 reward forever. Like in [Topin et al. \(2021\)](#), we
 729 use the gymnasium CartPole-v0 implementation [Towers et al. \(2024\)](#) of the CartPole MDP in
 730 which trajectories are truncated after 200 timesteps making the maximum cumulative reward, i.e.
 731 the optimal value of the RL objective when $\gamma = 1$, to be 200. The state features of the CartPole
 732 MDP are in $[-2, 2] \times [-2, 2] \times [-0.14, 0.14] \times [-1.4, 1.4]$.

733 **IBMDP** Authors define the associated IBMDP (definition 5) with $\zeta = -0.01$ and 4 information
 734 gathering actions. In addition to the original IBMDP paper, we also try $\zeta = 0.01$ and 3 information
 735 gathering actions. We use the same discount factor as the authors: $\gamma = 1$. We try two different
 736 approaches to limit the depth of decision tree policies to be at most 2: terminating trajectories if the
 737 agent takes too many information gathering actions in a row or simply giving a reward of -1 to the
 738 agent every time it takes an information gathering action past the depth limit. In practice, we could
 739 have tried an action masking approach, i.e. having a state dependent-action set, but we want to abide
 740 to the MDP formalism in order to properly understand direct interpretable approaches. We will also
 741 try IBMDPs where we do not limit the maximum depth for completeness.

Table 3: (Modified) PPO trained on 4×10^6 timesteps. This gives two different instantiation of (modified) PPO. Hyperparameters not mentioned are stable-baselines3 default. In green we highlight the hyperparameters from the original paper and in red we highlight the hyperparameter names for which author do not give information.

Hyperparameter	Values
Steps between each policy gradient steps	512
Number of minibatch for policy gradient updates	4
Networks architectures	[64, 64]
Networks activations	tanh(), relu()

Table 4: Top 5 hyperparameter configurations for modified DQN + IBMDP, bold font represent the original paper hyperparameters.

Rank	q	Depth control	Activation	Exploration	ζ	Mean Final Performance
1	3	termination	tanh	0.9	0.01	53
2	2	termination	tanh	0.5	-0.01	24
3	3	termination	tanh	0.5	-0.01	24
4	2	termination	tanh	0.5	0.01	23
5	2	termination	tanh	0.9	-0.01	22

742 In tables 4 and 5 we report the top-5 hyperparameters for Modified RL baselines when learning
743 partially observable IBMDP policies in terms of extracted decision tree policies performances in the
744 CartPole MDP.

745 9.2 Experimental setup

746 **Modified DQN and Modified PPO** as mentioned above, the authors use the modified version of
747 DQN from algorithm 2. We use the exact same hyperparameters for modified DQN as the authors
748 when possible. We use the same layers width (128) and number of hidden layers (2), the same
749 exploration strategy (ϵ -greedy with linearly decreasing value ϵ between 0.5 and 0.05 during the
750 first 10% of the training), the same replay buffer size (10^6) and the same number of transitions
751 to be collected randomly before doing value updates (10^5). We also try to use more exploration
752 during training (change the initial ϵ value to 0.9). We use the same optimizer (RMSprop with
753 hyperparameter 0.95 and learning rate 2.5×10^{-4}) to update the Q -networks. Authors did not share
754 which DQN implementation they used so we use the stable-baselines3 one Raffin et al. (2021)³.
755 Authors did not share which activation functions they used so we try both tanh and relu. For the
756 modified PPO algorithm (algorithm 3), we can exactly match the authors hyperparameters since they

³We are cleaning our source code and will open source it as soon as possible

Table 5: Top 5 hyperparameter configurations for modified PPO + IBMDP, bold font represent the original paper hyperparameters.

Rank	q	Depth Control	Activation	ζ	Mean Final Performance
1	3	reward	relu	0.01	139
2	3	termination	relu	0.01	132
3	3	reward	tanh	-0.01	119
4	3	reward	relu	-0.01	117
5	3	reward	tanh	0.01	116

Data: IBMDP $\mathcal{M}_{IB}\langle S \times O, A \cup A_{info}, (R, \zeta), (T, T_0, T_{info}) \rangle$, learning rate α , exploration rate ϵ , partially observable Q-network parameters θ , Q-network parameters ϕ , replay buffer \mathcal{B} , update frequency C

Result: deterministic memoryless policy π_{po}

Initialize partially observable Q-network parameters θ

Initialize Q-network parameters ϕ and target network parameters $\phi^- = \phi$

Initialize replay buffer $\mathcal{B} = \emptyset$

for each episode **do**

- Initialize downstream state features $s_0 \sim T_0$
- Initialize observation $\mathbf{o}_0 = (L_1, U_1, \dots, L_p, U_p)$
- for** each step t **do**

 - Choose action a_t using ϵ -greedy: $a_t = \text{argmax}_a Q_\theta(\mathbf{o}_t, a)$ with prob. $1 - \epsilon$
 - Take action a_t , observe r_t
 - Store transition $(s_t, \mathbf{o}_t, a_t, r_t, s_{t+1})$ in \mathcal{B}
 - Sample random batch $(\mathbf{s}_i, \mathbf{o}_i, a_i, r_i, s_{i+1}) \sim \mathcal{B}$
 - $a' = \underset{a}{\text{argmax}} Q_\theta(\mathbf{o}_i, a)$
 - $y_i = r_i + \gamma Q_{\phi^-}(\mathbf{s}_{i+1}, a')$ // Compute target $\phi \leftarrow \phi - \alpha \nabla_\phi (Q_\phi(\mathbf{s}_i, a_i) - y_i)^2$ // Update Q-network
 - $\theta \leftarrow \theta - \alpha \nabla_\theta (Q_\theta(\mathbf{o}_i, a_i) - y_i)^2$ // Update partially observable Q-network
 - if** $t \bmod C = 0$ **then**

 - $\theta^- \leftarrow \theta$ // Update target network

 - end**
 - $s_t \leftarrow s_{t+1}$
 - $\mathbf{o}_t \leftarrow \mathbf{o}_{t+1}$

- end**
- $\pi_{po}(\mathbf{o}) = \text{argmax}_a Q_\theta(\mathbf{o}, a)$ // Extract greedy policy

Algorithm 2: Modified Deep Q-Network. We highlight in green the changes to the standard DQN Mnih et al. (2015).

Data: IBMDP $\mathcal{M}_{IB}\langle S \times O, A \cup A_{info}, (R, \zeta), (T, T_0, T_{info}) \rangle$, learning rate α , policy parameters θ , clipping parameter ϵ , value function parameters ϕ

Result: Memoryless stochastic policy π_{po_θ}

Initialize policy parameters θ and value function parameters ϕ

for each episode **do**

- Generate trajectory $\tau = (s_0, \mathbf{o}_0, a_0, r_0, s_1, \mathbf{o}_1, a_1, r_1, \dots)$ following π_θ
- for** each timestep t in trajectory **do**

 - $G_t \leftarrow \sum_{k=t}^T \gamma^{k-t} r_k$ // Compute return
 - $A_t \leftarrow G_t - V_\phi(s_t)$ // Compute advantage
 - $r_t(\theta) \leftarrow \frac{\pi_{po_\theta}(a_t | \mathbf{o}_t)}{\pi_{po_\theta old}(a_t | \mathbf{o}_t)}$ // Compute probability ratio
 - $L_t^{CLIP} \leftarrow \min(r_t(\theta) A_t, \text{clip}(r_t(\theta), 1 - \epsilon, 1 + \epsilon) A_t)$ // Clipped objective
 - $\theta \leftarrow \theta + \alpha \nabla_\theta L_t^{CLIP}$ // Policy update
 - $\phi \leftarrow \phi + \alpha \nabla_\phi (G_t - V_\phi(s_t))^2$ // Value function update

- end**
- $\theta_{old} \leftarrow \theta$ // Update old policy

end

Algorithm 3: Modified Proximal Policy Optimization

757 use the open source stable-baselines3 implementation of PPO. We match training budgets: we train
758 modified DQN on 1 million timesteps and modified PPO on 4 million timesteps.

759 **DQN and PPO** We also benchmark the standard DQN and PPO when learning standard Marko-
760 vian IBMDP policies $\pi : S \times O \rightarrow A \cup A_{info}$ and when learning standard $\pi : S \rightarrow A$ policies
761 directly in the CartPole MDP. We summarize hyperparameters for the IBMDP and for the learning
762 algorithms in appendices 1, 2 and 3.

763 **Indirect methods** We also compare modified RL algorithm to imitation learning. To do so, we use
764 VIPER or Dagger to imitate greedy neural network policies obtained with standard DQN learning
765 directly on CartPole. We use Dagger to imitate neural network policies obtained with the standard
766 PPO learning directly on CartPole. For each indirect method, we imitate the neural network experts
767 by fitting decision trees on 10000 expert transitions using the CART Breiman et al. (1984) imple-
768 mentation from scikit-learn Pedregosa et al. (2011) with default hyperparameters and maximum
769 depth of 2 like in Topin et al. (2021).

770 **9.2.1 Metrics**

771 The key metric of this section is performance when controlling the CartPole, i.e., the average *undis-
772 counted* cumulative reward of a policy on 100 trajectories (RL objective with $\gamma = 1$). For modified
773 RL algorithms that learn a memoryless policy (or Q -function) in an IBMDP, we periodically extract
774 the policy (or Q -function) and use algorithm 1 to extract a decision tree for the CartPole MDP. We
775 then evaluate the tree on 100 independent trajectories in the MDP and report the mean undiscounted
776 cumulative reward. For RL applied to IBMDPs, since we can't deploy learned policies directly to
777 the downstream MDP as the state dimensions mismatch—such policies are $S \times O \rightarrow A \cup A_{info}$ but
778 the MDP states are in S —we periodically evaluate those IBMDP policies in a copy of the IBMDP in
779 which we fix $\zeta = 0$ ensuring that the copied IBMDP undiscounted cumulative rewards only account
780 rewards from the CartPole MDP (non-zero rewards in the IBMDP only occur when a reward from
781 the downstream MDP is given, i.e. when $a_t \in A$ in the IBMDP (definition 5)). Similarly, we do
782 100 trajectories of the extracted policies in the copied IBMDP and report the average undiscounted
783 cumulative reward. For RL applied directly to the downstream MDP we can just periodically extract
784 the learned policies and evaluate them on 100 CartPole trajectories.

785 Since imitation learning baselines train offline, i.e., on a fixed dataset, their performances cannot
786 directly be reported on the same axis as RL baselines. For that reason, during the training of a
787 standard RL baseline, we periodically extract the trained neural policy/ Q -function that we consider
788 as the expert to imitate. Those experts are then imitated with VIPER or Dagger using 10 000
789 newly generated transitions and then fitted decision tree policies are then evaluated on 100 CartPole
790 trajectories. We do not report the imitation learning objective values during VIPER or Dagger
791 training. Every single combination of IBMDP and Modified RL hyperparameters is run 20 times.
792 For standard RL on either an IBMDP or an MDP, we use the paper original hyperparameters when
793 they were specified, with depth control using negative rewards, $tanh()$ activations. We use 20
794 individual random seeds for every experiment in this chapter. Next, we present our results when
795 reproducing Topin et al. (2021).

796 **9.3 Results**

797 **9.3.1 How well do modified deep RL baselines learn in IBMDPs?**

798 On figure 9a, we observe that modified DQN can learn in IBMDPs—the curves have an increasing
799 trend—but we also observe that modified DQN finds poor decision tree policies for the CartPole MDP
800 in average—the curves flatten at the end of the x-axis and have low y-values. In particular, the highest
801 final y-value, among all the learning curves that could possibly correspond to the original paper
802 modified DQN, correspond to poor performances on the CartPole MDP. On figure 9b, we observe
803 that modified PPO finds decision tree policies with almost 150 cumulative rewards towards the end

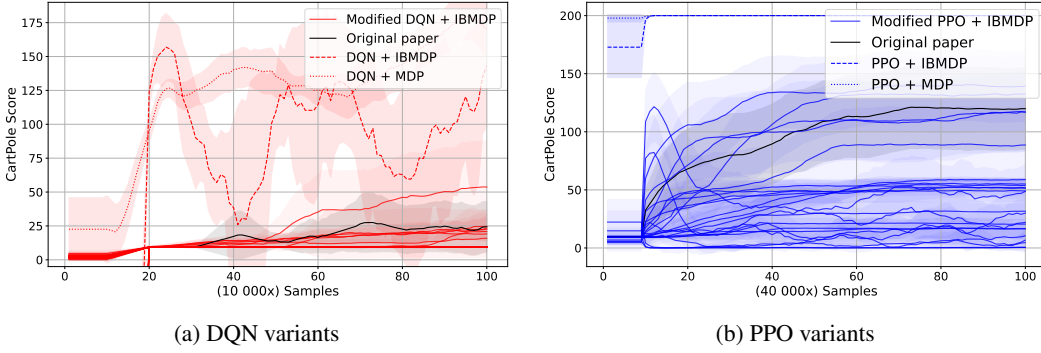


Figure 9: Comparison of modified reinforcement learning algorithms on different CartPole IBMDPs. (a) Shows variations of modified DQN and DQN (table 2), while (b) shows variations of modified PPO and PPO (table 3). For both algorithms, we give different line-styles for the learning curves when applied directly on the CartPole MDP versus when applied on the IBMDP to learn standard Markovian policies. We color the modified RL algorithm variant from the original paper in black. Shaded areas represent the confidence interval at 95% at each measure on the y-axis.

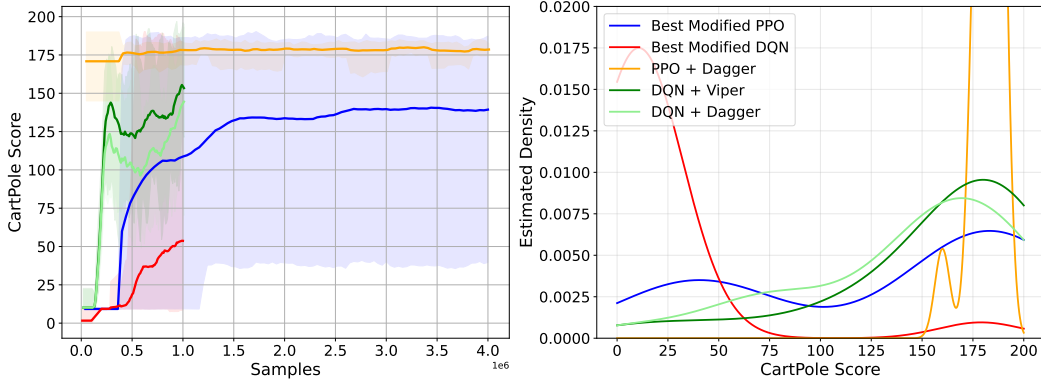


Figure 10: (left) Mean performance of the best-w.r.t. the RL objective for CartPole-modified RL + IBMDP combination. Shaded areas represent the min and max performance over the 20 seeds during training. (right) Corresponding score distribution of the final decision tree policies w.r.t. the RL objective for CartPole.

804 of training. The performance difference with modified DQN could be because we trained modified
 805 PPO longer, like in the original paper. However it could also be because DQN-like algorithms with
 806 those hyperparameters struggle to learn in CartPole (IB)MDPs. Indeed, we notice that for DQN-like
 807 baselines, learning seems difficult in general independently of the setting. On figures 9a and 9b, we
 808 observe that standard RL baselines (RL + IBMDP and RL + MDP), learn better CartPole policies
 809 in average than their modified counterparts that learn memoryless policies. On figure 9b, it is clear
 810 that for the standard PPO baselines, learning is super efficient and algorithms learn optimal policies
 811 with reward 200 in few thousands steps.

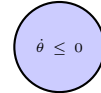
812 **9.3.2 Which decision tree policies does direct reinforcement learning return for the
 813 CartPole MDP?**

814 On figure 10, we isolate the best performing algorithms instantiations that learn decision tree poli-
 815 cies for the CartPole MDP. We compare the best modified DQN and modified PPO to imitation
 816 learning baselines that use the surrogate imitation objective to find CartPole decision tree policies.
 817 We find that despite having poor performances in *average*, the modified deep reinforcement learning

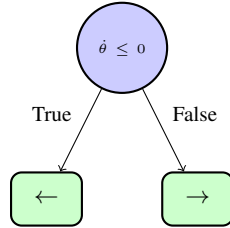
Most frequent modified PPO tree (12)



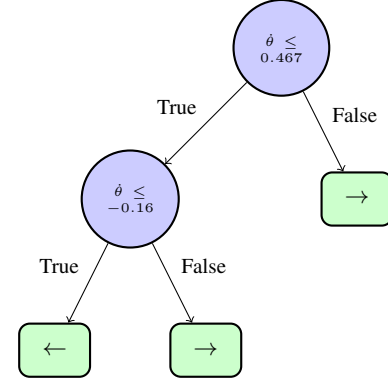
Most frequent modified DQN tree (9.5)



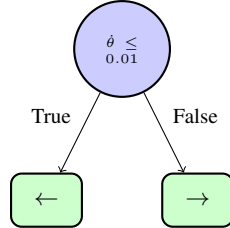
Best modified PPO tree (175)



Best modified DQN tree (160)



Typical imitated tree (185)



Best DQN + VIPER tree (200)

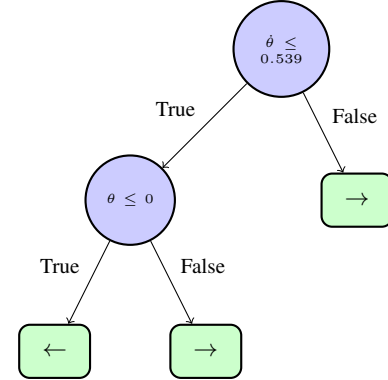


Figure 11: Trees obtained by modified deep RL in IBMDPs against trees obtained with imitation (RL objective value). θ and $\dot{\theta}$ are respectively the angle and the angular velocity of the pole

818 baselines can find very good decision tree policies as shown by the min-max shaded areas on the
 819 left of figure 10 and the corresponding estimated density of learned trees performances. However
 820 this is not desirable, a user typically wants an algorithm that can consistently find good decision
 821 tree policies. As shown by the estimated densities, indirect methods consistently find good decision
 822 tree policies (the higher modes of distributions are on the right of the plot). On the other hand, the
 823 decision tree policies returned by direct RL methods seem equally distributed on both extremes of
 824 the scores.

825 On figure 11, we present the best decision tree policies for CartPole returned by modified DQN and
 826 modified PPO. We used algorithm 1 to extract 20 trees from the 20 memoryless policies returned by
 827 the modified deep reinforcement learning algorithms over the 20 training seeds. We then plot the best
 828 tree for each baseline. Those trees get an average RL objective of roughly 175. Similarly, we plot a
 829 representative tree for imitation learning baseline as well as a tree that is optimal for CartPole w.r.t.
 830 the RL objective obtained with VIPER. Unlike for direct methods, the trees returned by imitation
 831 learning are extremely similar across seeds. In particular they often only vary in the scalar value
 832 used in the root node but in general have the same structure and test the angular velocity. On the
 833 other hand the most frequent trees across seeds returned by modified RL baselines are “trivial”
 834 decision tree policies that either repeat the same downstream action forever or repeat the same IGA
 835 (definition 5) forever.

836 10 RL objective values calculations

837 **Optimal depth-1 decision tree policy** $\pi_{\mathcal{T}_1}$ has one root node that tests $x \leq 1$ (respectively $y \leq 1$)
 838 and two leaf nodes \rightarrow and \downarrow . To compute $V_{\mathcal{T}_1}^{\pi}(o_0)$, we compute the values of $\pi_{\mathcal{T}_1}$ in each of the
 839 possible starting states $(s_0, o_0), (s_1, o_0), (s_2, o_0), (s_g, o_0)$ and compute the expectation over those.
 840 At initialization, when the downstream state is $s_g = (1.5, 0.5)$, the depth-1 decision tree policy
 841 cycles between taking an information gathering action $x \leq 1$ and moving down to get a positive
 842 reward for which it gets the returns:

$$\begin{aligned} V^{\pi_{\mathcal{T}_1}}(s_g, o_0) &= \zeta + \gamma + \gamma^2 \zeta + \gamma^3 \dots \\ &= \sum_{t=0}^{\infty} \gamma^{2t} \zeta + \sum_{t=0}^{\infty} \gamma^{2t+1} \\ &= \frac{\zeta + \gamma}{1 - \gamma^2} \end{aligned}$$

843 At initialization, in either of the downstream states $s_0 = (0.5, 0.5)$ and $s_2 = (1.5, 1.5)$, the value of
 844 the depth-1 decision tree policy is the return when taking one information gathering action $x \leq 1$,
 845 then moving right or down, then following the policy from the goal state s_g :

$$\begin{aligned} V^{\pi_{\mathcal{T}_1}}(s_0, o_0) &= \zeta + \gamma 0 + \gamma^2 V^{\pi_{\mathcal{T}_1}}(s_g, o_0) \\ &= \zeta + \gamma^2 V^{\pi_{\mathcal{T}_1}}(s_g, o_0) \\ &= V^{\pi_{\mathcal{T}_1}}(s_2, o_0) \end{aligned}$$

846 Similarly, the value of the best depth-1 decision tree policy in state $s_1 = (0.5, 1.5)$ is the value of
 847 taking one information gathering action then moving right to s_2 then following the policy in s_2 :

$$\begin{aligned} V^{\pi_{\mathcal{T}_1}}(s_1, o_0) &= \zeta + \gamma 0 + \gamma^2 V^{\pi_{\mathcal{T}_1}}(s_2, o_0) \\ &= \zeta + \gamma^2 V^{\pi_{\mathcal{T}_1}}(s_2, o_0) \\ &= \zeta + \gamma^2 (\zeta + \gamma^2 V^{\pi_{\mathcal{T}_1}}(s_g, o_0)) \\ &= \zeta + \gamma^2 \zeta + \gamma^4 V^{\pi_{\mathcal{T}_1}}(s_g, o_0) \end{aligned}$$

848 Since the probability of being in any downstream states at initialization given that the observation is
 849 \mathbf{o}_0 is simply the probability of being in any downstream states at initialization, we can write:

$$\begin{aligned} V^{\pi_{\mathcal{T}_1}}(\mathbf{o}_0) &= \frac{1}{4}V^{\pi_{\mathcal{T}_1}}(\mathbf{s}_g, \mathbf{o}_0) + \frac{2}{4}V^{\pi_{\mathcal{T}_1}}(\mathbf{s}_2, \mathbf{o}_0) + \frac{1}{4}V^{\pi_{\mathcal{T}_1}}(\mathbf{s}_1, \mathbf{o}_0) \\ &= \frac{1}{4}\frac{\zeta + \gamma}{1 - \gamma^2} + \frac{2}{4}(\zeta + \gamma^2)\frac{\zeta + \gamma}{1 - \gamma^2} + \frac{1}{4}(\zeta + \gamma^2\zeta + \gamma^4)\frac{\zeta + \gamma}{1 - \gamma^2} \\ &= \frac{1}{4}\frac{\zeta + \gamma}{1 - \gamma^2} + \frac{2}{4}\frac{(\zeta + \gamma^3)}{1 - \gamma^2} + \frac{1}{4}\frac{(\zeta + \gamma^5)}{1 - \gamma^2} \\ &= \frac{4\zeta + \gamma + 2\gamma^3 + \gamma^5}{4(1 - \gamma^2)} \end{aligned}$$

850 **Depth-0 decision tree:** has only one leaf node that takes a single downstream action indefinitely.
 851 For this type of tree the best reward achievable is to take actions that maximize the probability of
 852 reaching the objective \rightarrow or \downarrow . In that case the objective value of such tree is: In the goal state
 853 $G = (1, 0)$, the value of the depth-0 tree \mathcal{T}_0 is:

$$\begin{aligned} V_G^{\mathcal{T}_0} &= 1 + \gamma + \gamma^2 + \dots \\ &= \sum_{t=0}^{\infty} \gamma^t \\ &= \frac{1}{1 - \gamma} \end{aligned}$$

854 In the state $(0, 0)$ when the policy repeats going right respectively in the state $(0, 1)$ when the policy
 855 repeats going down, the value is:

$$\begin{aligned} V_{S_0}^{\mathcal{T}_0} &= 0 + \gamma V_g^{\mathcal{T}_0} \\ &= \gamma V_G^{\mathcal{T}_0} \end{aligned}$$

856 In the other states the policy never gets positive rewards; $V_{S_1}^{\mathcal{T}_0} = V_{S_2}^{\mathcal{T}_0} = 0$. Hence:

$$\begin{aligned} J(\mathcal{T}_0) &= \frac{1}{4}V_G^{\mathcal{T}_0} + \frac{1}{4}V_{S_0}^{\mathcal{T}_0} + \frac{1}{4}V_{S_1}^{\mathcal{T}_0} + \frac{1}{4}V_{S_2}^{\mathcal{T}_0} \\ &= \frac{1}{4}V_G^{\mathcal{T}_0} + \frac{1}{4}\gamma V_G^{\mathcal{T}_0} + 0 + 0 \\ &= \frac{1}{4}\frac{1}{1 - \gamma} + \frac{1}{4}\gamma\frac{1}{1 - \gamma} \\ &= \frac{1 + \gamma}{4(1 - \gamma)} \end{aligned}$$

857 **Unbalanced depth-2 decision tree:** the unbalanced depth-2 decision tree takes an information
 858 gathering action $x \leq 0.5$ then either takes the \downarrow action or takes a second information $y \leq 0.5$
 859 followed by \rightarrow or \downarrow . In states G and S_2 , the value of the unbalanced tree is the same as for the
 860 depth-1 tree. In states S_0 and S_1 , the policy takes two information gathering actions before taking a
 861 downstream action and so on:

$$V_{S_0}^{\mathcal{T}_u} = \zeta + \gamma\zeta + \gamma^2 0 + \gamma^3 V_G^{\mathcal{T}_1}$$

862

$$\begin{aligned} V_{S_1}^{\mathcal{T}_u} &= \zeta + \gamma\zeta + \gamma^2 0 + \gamma^3 V_{S_0}^{\mathcal{T}_u} \\ &= \zeta + \gamma\zeta + \gamma^2 0 + \gamma^3(\zeta + \gamma\zeta + \gamma^2 0 + \gamma^3 V_G^{\mathcal{T}_1}) \\ &= \zeta + \gamma\zeta + \gamma^3\zeta + \gamma^4\zeta + \gamma^6 V_G^{\mathcal{T}_1} \end{aligned}$$

863 We get:

$$\begin{aligned}
 J(\mathcal{T}_u) &= \frac{1}{4}V_G^{\mathcal{T}_u} + \frac{1}{4}V_{S_0}^{\mathcal{T}_u} + \frac{1}{4}V_{S_1}^{\mathcal{T}_u} + \frac{1}{4}V_{S_2}^{\mathcal{T}_u} \\
 &= \frac{1}{4}V_G^{\mathcal{T}_1} + \frac{1}{4}(\zeta + \gamma\zeta + \gamma^3V_G^{\mathcal{T}_1}) + \frac{1}{4}(\zeta + \gamma\zeta + \gamma^3\zeta + \gamma^4\zeta + \gamma^6V_G^{\mathcal{T}_1}) + \frac{1}{4}V_{S_2}^{\mathcal{T}_1} \\
 &= \frac{1}{4}\left(\frac{\zeta + \gamma}{1 - \gamma^2}\right) + \frac{1}{4}\left(\frac{\gamma\zeta + \gamma^4 + \zeta - \gamma^2\zeta}{1 - \gamma^2}\right) + \frac{1}{4}(\zeta + \gamma\zeta + \gamma^3\zeta + \gamma^4\zeta + \gamma^6V_G^{\mathcal{T}_1}) + \frac{1}{4}V_{S_2}^{\mathcal{T}_1} \\
 &= \frac{1}{4}\left(\frac{\zeta + \gamma}{1 - \gamma^2}\right) + \frac{1}{4}\left(\frac{\gamma\zeta + \gamma^4 + \zeta - \gamma^2\zeta}{1 - \gamma^2}\right) + \frac{1}{4}\left(\frac{\zeta + \gamma\zeta - \gamma^2\zeta - \gamma^5\zeta + \gamma^6\zeta + \gamma^7}{1 - \gamma^2}\right) + \frac{1}{4}V_{S_2}^{\mathcal{T}_1} \\
 &= \frac{1}{4}\left(\frac{\zeta + \gamma}{1 - \gamma^2}\right) + \frac{1}{4}\left(\frac{\gamma\zeta + \gamma^4 + \zeta - \gamma^2\zeta}{1 - \gamma^2}\right) + \frac{1}{4}\left(\frac{\zeta + \gamma\zeta - \gamma^2\zeta - \gamma^5\zeta + \gamma^6\zeta + \gamma^7}{1 - \gamma^2}\right) + \frac{1}{4}\left(\frac{\zeta + \gamma^3}{1 - \gamma^2}\right) \\
 &= \frac{\zeta(4 + 2\gamma - 2\gamma^2 - \gamma^5 + \gamma^6) + \gamma + \gamma^3 + \gamma^4 + \gamma^7}{4(1 - \gamma^2)}
 \end{aligned}$$

864 **The balanced depth-2 decision tree:** alternates in every state between taking the two available
865 information gathering actions and then a downstream action. The value of the policy in the goal
866 state is:

$$\begin{aligned}
 V_G^{\mathcal{T}_2} &= \zeta + \gamma\zeta + \gamma^2 + \gamma^3\zeta + \gamma^4\zeta + \dots \\
 &= \sum_{t=0}^{\infty} \gamma^{3t}\zeta + \sum_{t=0}^{\infty} \gamma^{3t+1}\zeta + \sum_{t=0}^{\infty} \gamma^{3t+2}\zeta \\
 &= \frac{\zeta}{1 - \gamma^3} + \frac{\gamma\zeta}{1 - \gamma^3} + \frac{\gamma^2}{1 - \gamma^3}
 \end{aligned}$$

867 Following the same reasoning for other states we find the objective value for the depth-2 decision
868 tree policy to be:

$$\begin{aligned}
 J(\mathcal{T}_2) &= \frac{1}{4}V_G^{\mathcal{T}_2} + \frac{2}{4}V_{S_2}^{\mathcal{T}_2} + \frac{1}{4}V_{S_1}^{\mathcal{T}_2} \\
 &= \frac{1}{4}V_G^{\mathcal{T}_2} + \frac{2}{4}(\zeta + \gamma\zeta + \gamma^20 + \gamma^3V_G^{\mathcal{T}_2}) + \frac{1}{4}(\zeta + \gamma\zeta + \gamma^20 + \gamma^3\zeta + \gamma^4\zeta + \gamma^50 + \gamma^6V_G^{\mathcal{T}_2}) \\
 &= \frac{\zeta(3 + 3\gamma) + \gamma^2 + \gamma^5 + \gamma^8}{4(1 - \gamma^3)}
 \end{aligned}$$

869 **Infinite tree:** we also consider the infinite tree policy that repeats an information gathering action
870 forever and has objective: $J(\mathcal{T}_{\text{inf}}) = \frac{\zeta}{1 - \gamma}$

871 **Stochastic policy:** the other non-trivial policy that can be learned by solving a partially observable
872 IBMDP is the stochastic policy that guarantees to reach G after some time: fifty percent chance to
873 do \rightarrow and fifty percent chance to do \downarrow . This stochastic policy has objective value:

$$\begin{aligned}
 V_G^{\text{stoch}} &= \frac{1}{1 - \gamma} \\
 V_{S_0}^{\text{stoch}} &= 0 + \frac{1}{2}\gamma V_G^{\text{stoch}} + \frac{1}{2}\gamma V_{S_1}^{\text{stoch}} \\
 V_{S_2}^{\text{stoch}} &= 0 + \frac{1}{2}\gamma V_G^{\text{stoch}} + \frac{1}{2}\gamma V_{S_1}^{\text{stoch}} = V_{S_0}^{\text{stoch}} \\
 V_{S_1}^{\text{stoch}} &= 0 + \frac{1}{2}\gamma V_{S_2}^{\text{stoch}} + \frac{1}{2}\gamma V_G^{\text{stoch}} = \frac{1}{2}\gamma V_{S_0}^{\text{stoch}} + \frac{1}{2}\gamma V_G^{\text{stoch}}
 \end{aligned}$$

874 Solving these equations:

$$\begin{aligned}
 V_{S_1}^{\text{stoch}} &= \frac{1}{2}\gamma V_{S_0}^{\text{stoch}} + \frac{1}{2}\gamma V_G^{\text{stoch}} \\
 &= \frac{1}{2}\gamma\left(\frac{1}{2}\gamma V_G^{\text{stoch}} + \frac{1}{2}\gamma V_{S_1}^{\text{stoch}}\right) + \frac{1}{2}\gamma V_G^{\text{stoch}} \\
 &= \frac{1}{4}\gamma^2 V_G^{\text{stoch}} + \frac{1}{4}\gamma^2 V_{S_1}^{\text{stoch}} + \frac{1}{2}\gamma V_G^{\text{stoch}} \\
 V_{S_1}^{\text{stoch}} - \frac{1}{4}\gamma^2 V_{S_1}^{\text{stoch}} &= \frac{1}{4}\gamma^2 V_G^{\text{stoch}} + \frac{1}{2}\gamma V_G^{\text{stoch}} \\
 V_{S_1}^{\text{stoch}}(1 - \frac{1}{4}\gamma^2) &= (\frac{1}{4}\gamma^2 + \frac{1}{2}\gamma)V_G^{\text{stoch}} \\
 V_{S_1}^{\text{stoch}} &= \frac{\frac{1}{4}\gamma^2 + \frac{1}{2}\gamma}{1 - \frac{1}{4}\gamma^2} V_G^{\text{stoch}} \\
 &= \frac{\gamma(\frac{1}{4}\gamma + \frac{1}{2})}{1 - \frac{1}{4}\gamma^2} \cdot \frac{1}{1 - \gamma} \\
 &= \frac{\gamma(\frac{1}{4}\gamma + \frac{1}{2})}{(1 - \frac{1}{4}\gamma^2)(1 - \gamma)}
 \end{aligned}$$

875

$$\begin{aligned}
 V_{S_0}^{\text{stoch}} &= \frac{1}{2}\gamma V_G^{\text{stoch}} + \frac{1}{2}\gamma V_{S_1}^{\text{stoch}} \\
 &= \frac{1}{2}\gamma \cdot \frac{1}{1 - \gamma} + \frac{1}{2}\gamma \cdot \frac{\gamma(\frac{1}{4}\gamma + \frac{1}{2})}{(1 - \frac{1}{4}\gamma^2)(1 - \gamma)} \\
 &= \frac{\frac{1}{2}\gamma}{1 - \gamma} + \frac{\frac{1}{2}\gamma^2(\frac{1}{4}\gamma + \frac{1}{2})}{(1 - \frac{1}{4}\gamma^2)(1 - \gamma)} \\
 &= \frac{\frac{1}{2}\gamma(1 - \frac{1}{4}\gamma^2) + \frac{1}{2}\gamma^2(\frac{1}{4}\gamma + \frac{1}{2})}{(1 - \frac{1}{4}\gamma^2)(1 - \gamma)} \\
 &= \frac{\frac{1}{2}\gamma - \frac{1}{8}\gamma^3 + \frac{1}{8}\gamma^3 + \frac{1}{4}\gamma^2}{(1 - \frac{1}{4}\gamma^2)(1 - \gamma)} \\
 &= \frac{\frac{1}{2}\gamma + \frac{1}{4}\gamma^2}{(1 - \frac{1}{4}\gamma^2)(1 - \gamma)} \\
 &= \frac{\gamma(\frac{1}{2} + \frac{1}{4}\gamma)}{(1 - \frac{1}{4}\gamma^2)(1 - \gamma)}
 \end{aligned}$$

876

$$\begin{aligned}
J(\mathcal{T}_{\text{stoch}}) &= \frac{1}{4}(V_G^{\text{stoch}} + V_{S_0}^{\text{stoch}} + V_{S_1}^{\text{stoch}} + V_{S_2}^{\text{stoch}}) \\
&= \frac{1}{4} \left(\frac{1}{1-\gamma} + 2 \cdot \frac{\gamma(\frac{1}{2} + \frac{1}{4}\gamma)}{(1 - \frac{1}{4}\gamma^2)(1-\gamma)} + \frac{\gamma(\frac{1}{4}\gamma + \frac{1}{2})}{(1 - \frac{1}{4}\gamma^2)(1-\gamma)} \right) \\
&= \frac{1}{4} \left(\frac{1}{1-\gamma} + \frac{2\gamma(\frac{1}{2} + \frac{1}{4}\gamma) + \gamma(\frac{1}{4}\gamma + \frac{1}{2})}{(1 - \frac{1}{4}\gamma^2)(1-\gamma)} \right) \\
&= \frac{1}{4} \left(\frac{1}{1-\gamma} + \frac{\gamma + \frac{1}{2}\gamma^2 + \frac{1}{4}\gamma^2 + \frac{1}{2}\gamma}{(1 - \frac{1}{4}\gamma^2)(1-\gamma)} \right) \\
&= \frac{1}{4} \left(\frac{1}{1-\gamma} + \frac{\frac{3}{2}\gamma + \frac{3}{4}\gamma^2}{(1 - \frac{1}{4}\gamma^2)(1-\gamma)} \right) \\
&= \frac{1}{4} \left(\frac{1 - \frac{1}{4}\gamma^2 + \frac{3}{2}\gamma + \frac{3}{4}\gamma^2}{(1 - \frac{1}{4}\gamma^2)(1-\gamma)} \right) \\
&= \frac{1}{4} \left(\frac{1 + \frac{3}{2}\gamma + \frac{1}{2}\gamma^2}{(1 - \frac{1}{4}\gamma^2)(1-\gamma)} \right) \\
&= \frac{1 + \frac{3}{2}\gamma + \frac{1}{2}\gamma^2}{4(1 - \frac{1}{4}\gamma^2)(1-\gamma)}
\end{aligned}$$

877 **11 Training curves**

878 We plot the sub-optimality gaps during training, w.r.t. the RL objective (definition 2),
879 between the learned memoryless policy and the optimal deterministic memoryless policy:
880 $|\mathbb{E}[V^{\pi^*}(s_0, o_0)|s_0 \sim T_0] - \mathbb{E}[V^\pi(s_0, o_0)|s_0 \sim T_0]|$. Because we know the whole POIBMDP
881 model that we can represent exactly as tables, and because we know for each ζ the RL objective value
882 of the optimal deterministic memoryless policy (figure 2), we can report the *exact* sub-optimality
883 gaps. In figure 12, we plot the sub-optimality gaps—averaged over 100 seeds—of learned policies
884 during training. We do so for 200 different POIBMDPs where we change the reward for informa-
885 tion gathering actions: we sample 200 ζ values uniformly in $[-1, 2]$. In figure 12, a different color
886 represents a different POIBMDP.

887 Recall from figure 2 that for: (i) $\zeta \in [-1, 0]$, the optimal deterministic memoryless policy is a depth-
888 0 tree, (ii) $\zeta \in]0, 1[$, the optimal deterministic memoryless policy is a depth-1 tree, and (iii) $\zeta \in [1, 2]$,
889 the optimal deterministic memoryless policy is a “infinite” tree that contains infinite number of
890 internal nodes. We observe that, despite all sub-optimality gaps converging independently of the ζ
891 values, not all algorithms in all POIBMDPs fully minimize the sub-optimality gap. In particular, all
892 algorithms seem to consistently minimize the gap, i.e. learn the optimal policy or Q-function, only
893 for $\zeta \in [1, 2]$ (all the yellow lines go to 0). However, we are interested in the range $\zeta \in]0, 1[$ where
894 the optimal decision tree policy is non-trivial, i.e. not taking the same action forever. In that range,
895 no baseline consistently minimizes the sub-optimality gap.

896 **12 Tabular RL algorithmic details for POIBMDPs**897 **12.1 Training with the best hyperparameters**898 **13 POIBMDPs for classification tasks**

899 Let us show that, POIBMDPs associated with MDPs encoding supervised learning tasks, are in fact
900 MDPs themselves. Let us define such supervised learning MDPs in the context of a classification
901 task (this definition extends trivially to regression tasks).

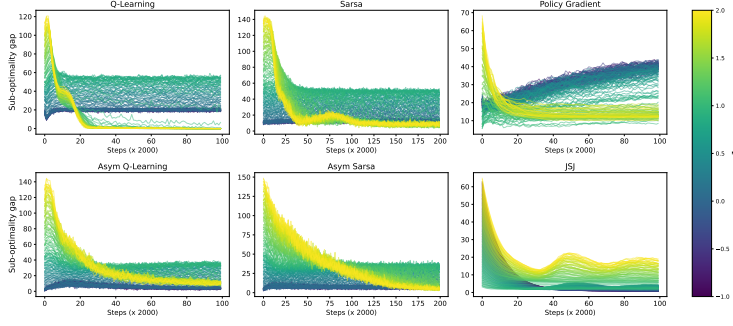


Figure 12: (Asymmetric) reinforcement learning in POIBMDPs. In each subplot, each single line is colored by the value of ζ in the corresponding POIBMDP in which learning occurs. Each single learning curve represent the sub-optimality gap averaged over 100 seeds.

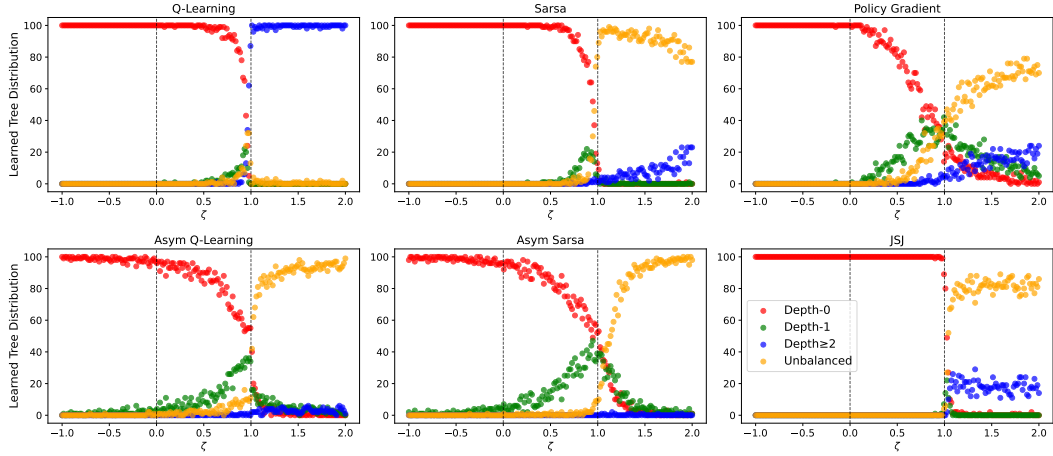
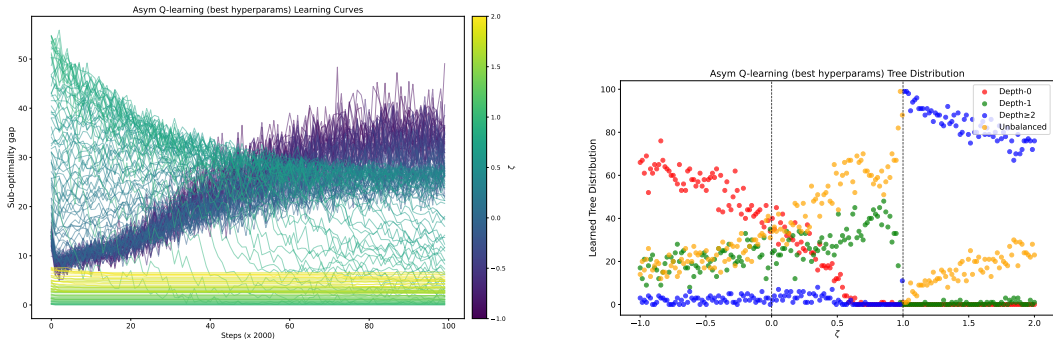


Figure 13: Distributions of final tree policies learned across the 100 seeds. For each ζ value, there are four colored points. Each point represent the share of depth-0 trees (red), depth-1 trees (green), unbalanced depth-2 trees (orange) and depth-2 trees (blue).



(a) Learning curves for asymmetric Q-learning with good hyperparameters.

(b) Trees distributions for asymmetric Q-learning with good hyperparameters

Figure 14: Analysis of the top-performing asymmetric Q-learning instantiation. (left) Learning curves, and (right) tree distributions across different POIBMDP configurations.

Algorithm 4: Asymmetric Q-Learning. We highlight in green the differences with the standard Q-learning [Watkins & Dayan \(1992\)](#)

Data: A POMDP, learning rates α_u, α_q , exploration prob. ϵ
Result: $\pi : O \rightarrow A$

Initialize $U(\mathbf{x}, a) = 0$ for all $\mathbf{x} \in X, a \in A$
 Initialize $Q(\mathbf{o}, a) = 0$ for all $\mathbf{o} \in O, a \in A$

for each episode do

- Initialize state $x_0 \sim T_0$
- Initialize observation $\mathbf{o}_0 \sim \Omega(x_0)$
- for each step t do**
 - Choose action a_t using ϵ -greedy: $a_t = \text{argmax}_a Q(\mathbf{o}_t, a)$ with prob. $1 - \epsilon$
 - Take action a_t , observe $r_t = R(\mathbf{x}_t, a_t)$, $x_{t+1} \sim T(x_t, a_t)$, and $\mathbf{o}_{t+1} \sim \Omega(x_{t+1})$
 - $y \leftarrow r + \gamma U(\mathbf{x}_{t+1}, \text{argmax}_{a'} Q(\mathbf{o}_{t+1}, a'))$
 - $U(\mathbf{x}_t, a_t) \leftarrow (1 - \alpha_u)U(\mathbf{x}_t, a_t) + \alpha_u y$
 - $Q(\mathbf{o}_t, a_t) \leftarrow (1 - \alpha_q)Q(\mathbf{o}_t, a_t) + \alpha_q y$
 - $x_t \leftarrow x_{t+1}$
 - $\mathbf{o}_t \leftarrow \mathbf{o}_{t+1}$
- end**

end

$\pi(o) = \text{argmax}_a Q(\mathbf{o}, a)$

Algorithm 5: Asymmetric Sarsa

Data: POMDP $\mathcal{M}_{po} = \langle X, O, A, R, T, T_0, \Omega \rangle$, learning rates α_u, α_q , exploration rate ϵ
Result: $\pi : O \rightarrow A$

Initialize $U(x, a) = 0$ for all $x \in X, a \in A$
 Initialize $Q(o, a) = 0$ for all $\mathbf{o} \in O, a \in A$

for each episode do

- Initialize state $x_0 \sim T_0$
- Initialize observation $\mathbf{o}_0 \sim \Omega(x_0)$
- Choose action a_0 using ϵ -greedy: $a_0 = \text{argmax}_a Q(\mathbf{o}_0, a)$ with prob. $1 - \epsilon$
- for each step t do**
 - Take action a_t , observe $r_t = R(x_t, a_t)$, $x_{t+1} \sim T(x_t, a_t)$, and $\mathbf{o}_{t+1} \sim \Omega(x_{t+1})$
 - Choose action a_{t+1} using ϵ -greedy: $a_{t+1} = \text{argmax}_a Q(\mathbf{o}_{t+1}, a)$ with prob. $1 - \epsilon$
 - $y \leftarrow r + \gamma U(x_{t+1}, a_{t+1}) // \text{ TD target using actual next action}$
 - $U(x_t, a_t) \leftarrow (1 - \alpha_u)U(x_t, a_t) + \alpha_u y$
 - $Q(\mathbf{o}_t, a_t) \leftarrow (1 - \alpha_q)Q(\mathbf{o}_t, a_t) + \alpha_q y$
 - $x_t \leftarrow x_{t+1}$
 - $\mathbf{o}_t \leftarrow \mathbf{o}_{t+1}$
 - $a_t \leftarrow a_{t+1}$
- end**

$\pi(\mathbf{o}) = \text{argmax}_a Q(\mathbf{o}, a) // \text{ Extract greedy policy}$

Algorithm 6: Asymmetric policy gradient algorithm. Uses Monte Carlo estimates of the average reward value functions to perform policy improvements.

Data: POMDP $\mathcal{M}_{po} = \langle X, O, A, R, T, T_0, \Omega \rangle$, learning rate α , policy parameters θ , number of trajectories N

Result: Stochastic partially observable policy $\pi_\theta : O \rightarrow \Delta(A)$

Initialize policy parameters θ

Initialize $Q(o, a) = 0$ for all observations o and actions a

for each episode do

- for** $i = 1$ to N **do**
 - Generate trajectory $\tau_i = (s_0, a_0, r_0, s_1, a_1, r_1, \dots, s_T)$ following π_θ
 - for each timestep** t **in trajectory** τ_i **do**
 - $G_t \leftarrow \sum_{k=t}^T \gamma^{k-t} r_k$ // Compute return
 - Store (o_t, a_t, G_t) for later averaging
 - end**
- end**
- for each unique observation-action pair** (o, a) **do**
 - $Q(o, a) \leftarrow \frac{1}{|\{(o, a)\}|} \sum_{(o, a, G)} G$ // Monte Carlo estimate
- end**
- for each observation** o **do**
 - for each action** a **do**
 - $\pi_1(a|o) \leftarrow 1.0$ if $a = \text{argmax}_{a'} Q(o, a')$, 0.0 otherwise // Deterministic policy from Q-values
 - $\pi(a|o) \leftarrow (1 - \alpha)\pi(a|o) + \alpha\pi_1(a|o)$ // Policy improvement step
 - end**
- end**
- Reset $Q(o, a) = 0$ for all observations o and actions a // Reset for next episode

end

Table 6: Summary of RL baselines Hyperparameters

algorithm	Problem	Hyperparameters comb.
Policy Gradient	PO/IB/MDP	420
JSJ	POIBMDP	15
Q-learning	PO/IB/MDP	192
Asym Q-learning	POIBMDP	768
Sarsa	PO/IB/MDP	192
Asym Sarsa	POIBMDP	768

Table 7: PG Hyperparameter Space (140 combinations)

Hyperparameter	Values	Description
Learning Rate (lr)	0.001, 0.005, 0.01, 0.05, 0.1	Policy gradient step size
Entropy Regularization (tau)	-1.0, -0.1, -0.01, 0.0, 0.01, 0.1, 1.0	Entropy regularization coefficient
Temperature (eps)	0.01, 0.1, 1.0, 10	Softmax temperature
Episodes per Update (n_steps)	20, 200, 2000	Number of episodes per policy update

Table 8: PG-IBMDP Hyperparameter Space (140 combinations)

Hyperparameter	Values	Description
Learning Rate (lr)	0.001, 0.005, 0.01, 0.05, 0.1	Policy gradient step size
Entropy Regularization (tau)	-1.0, -0.1, -0.01, 0.0, 0.01, 0.1, 1.0	Entropy regularization coefficient
Temperature (eps)	0.01, 0.1, 1.0, 10	Softmax temperature
Episodes per Update (n_steps)	10, 100, 1000	Number of episodes per policy update

Table 9: QL Hyperparameter Space (192 combinations)

Hyperparameter	Values	Description
Epsilon Schedules	(0.3, 1), (0.3, 0.99), (1, 1)	Initial exploration and decrease rate
Epsilon Schedules	(0.1, 1), (0.1, 0.99), (0.3, 0.99)	Initial exploration and decrease rate
Lambda	0.0, 0.3, 0.6, 0.9	Eligibility trace decay
Learning Rate (lr_o)	0.001, 0.005, 0.01, 0.1	Observation Q-learning rate
Optimistic	True, False	Optimistic initialization

Table 10: QL-Asym Hyperparameter Space (768 combinations)

Hyperparameter	Values	Description
Epsilon Schedules	(0.3, 1), (0.3, 0.99), (1, 1)	Initial exploration and decrease rate
Epsilon Schedules	(0.1, 1), (0.1, 0.99), (0.3, 0.99)	Initial exploration and decrease rate
Lambda	0.0, 0.3, 0.6, 0.9	Eligibility trace decay
Learning Rate (lr_o)	0.001, 0.005, 0.01, 0.1	Observation Q-learning rate
Learning Rate (lr_v)	0.001, 0.005, 0.01, 0.1	State-action Q-learning rate
Optimistic	True, False	Optimistic initialization

Table 11: QL-IBMDP Hyperparameter Space (192 combinations)

Hyperparameter	Values	Description
Epsilon Schedules	(0.3, 1), (0.3, 0.99), (1, 1)	Initial exploration and decrease rate
Epsilon Schedules	(0.1, 1), (0.1, 0.99), (0.3, 0.99)	Initial exploration and decrease rate
Lambda	0.0, 0.3, 0.6, 0.9	Eligibility trace decay
Learning Rate (lr_v)	0.001, 0.005, 0.01, 0.1	State-action Q-learning rate
Optimistic	True, False	Optimistic initialization

Table 12: SARSA Hyperparameter Space (192 combinations)

Hyperparameter	Values	Description
Epsilon Schedules	(0.3, 1), (0.3, 0.99), (1, 1)	Initial exploration and decrease rate
Epsilon Schedules	(0.1, 1), (0.1, 0.99), (0.3, 0.99)	Initial exploration and decrease rate
Lambda	0.0, 0.3, 0.6, 0.9	Eligibility trace decay
Learning Rate (lr_o)	0.001, 0.005, 0.01, 0.1	Observation SARSA learning rate
Optimistic	True, False	Optimistic initialization

Table 13: SARSA-Asym Hyperparameter Space (768 combinations)

Hyperparameter	Values	Description
Epsilon Schedules	(0.3, 1), (0.3, 0.99), (1, 1)	Initial exploration and decrease rate
Epsilon Schedules	(0.1, 1), (0.1, 0.99), (0.3, 0.99)	Initial exploration and decrease rate
Lambda	0.0, 0.3, 0.6, 0.9	Eligibility trace decay
Learning Rate (lr_o)	0.001, 0.005, 0.01, 0.1	Observation SARSA learning rate
Learning Rate (lr_v)	0.001, 0.005, 0.01, 0.1	State-action SARSA learning rate
Optimistic	True, False	Optimistic initialization

Table 14: SARSA-IBMDP Hyperparameter Space (192 combinations)

Hyperparameter	Values	Description
Epsilon Schedules	(0.3, 1), (0.3, 0.99), (1, 1)	Initial exploration and decrease rate
Epsilon Schedules	(0.1, 1), (0.1, 0.99), (0.3, 0.99)	Initial exploration and decrease rate
Lambda	0.0, 0.3, 0.6, 0.9	Eligibility trace decay
Learning Rate (lr_v)	0.001, 0.005, 0.01, 0.1	State-action SARSA learning rate
Optimistic	True, False	Optimistic initialization

Table 15: Asymmetric sarsa hyperparameters (768 combinations each run 10 times)

Hyperparameter	Values	Description
Epsilon Schedules	(0.3, 1), (0.3, 0.99), (1, 1)	Initial exploration and decrease rate
Epsilon Schedules	(0.1, 1), (0.1, 0.99), (0.3, 0.99)	Initial exploration and decrease rate
Lambda	0.0, 0.3, 0.6, 0.9	Eligibility trace decay
Learning Rate U	0.001, 0.005, 0.01, 0.1	learning rate for the Q-function
Learning Rate Q	0.001, 0.005, 0.01, 0.1	learning rate for the partial observation dependent Q-function
Optimistic	True, False	Optimistic initialization

Hyperparameter	Asym Q-learning (10/10)	Asym Sarsa (10/10)	PG (4/10)
epsilon_start	1.0	1.0	-
epsilon_decay	0.99	0.99	-
batch_size	1	1	-
lambda_	0.0	0.0	-
lr_o	0.01	0.1	-
lr_v	0.1	0.005	-
optimistic	False	False	-
lr	-	-	0.05
tau	-	-	0.1
eps	-	-	0.1
n_steps	-	-	2000

Table 16: Best hyperparameters for each algorithm on the POIBMDP problem

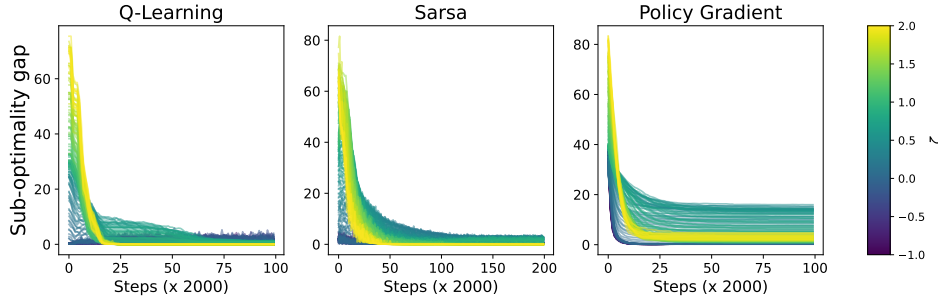


Figure 15: We reproduce the same plot as in figure 12 for classification POIBMDPs. Each individual curve is the sub-optimality gap of the learned policy during training averaged over 100 runs for a single ζ value.

902 **Definition 9** (Classification Markov decision process). Given a set of N examples denoted $\mathcal{E} =$
 903 $\{(\mathbf{x}_i, y_i)\}_{i=1}^N$ where each datum $\mathbf{x}_i \in \mathcal{X}$ is described by a set of p features x_{ij} with $1 \leq j \leq p$,
 904 and $y_i \in \mathbb{Z}^m$ is the label associated with \mathbf{x}_i , a classification Markov decision Process is an MDP
 905 $\langle S, A, R, T, T_0 \rangle$ (definition 1). The state space is $S = \{\mathbf{x}_i\}_{i=1}^N$, the set of training data features.
 906 The action space is $A = \mathbb{Z}^m$, the set of unique labels. The reward function is $R : S \times A \rightarrow \{0, 1\}$
 907 with $R(\mathbf{s} = \mathbf{x}_i, a) = 1_{\{a=y_i\}}$. The transition function is $T : S \times A \rightarrow \Delta(S)$ with $T(\mathbf{s}, a, \mathbf{s}') =$
 908 $\frac{1}{N} \forall s, a, s'$. The initial distribution is $T_0(\mathbf{s}_0 = \mathbf{s}) = \frac{1}{N}$.

909 One can be convinced that policies that maximize the RL objective (definition 2) in classifi-
 910 cation MDPs are classifiers that maximize the prediction accuracy because $\sum_{i=1}^N 1_{\pi(\mathbf{x}_i)=y_i} =$
 911 $\sum_{i=1}^N R(\mathbf{x}_i, \pi(\mathbf{x}_i))$. We defer the formal proof in the next part of the manuscript in which we
 912 extensively study supervised learning problems.

913 Now let us show that associated POIBMDPs are in fact MDPs. We show this by construction.

914 **Definition 10** (Classification POIBMDP). Given a classification MDP $\langle \{\mathbf{x}_i\}_{i=1}^N, \mathbb{Z}^m, R, T, T_0 \rangle$
 915 (definition 9), and an associated POIBMDP $\langle S, O, A, A_{info}, R, \zeta, T_{info}, T, T_0 \rangle$ (definition 7), a
 916 classification POIBMDP is an MDP (definition 1):

$$\langle \overbrace{O}^{\text{State space}}, \overbrace{\mathbb{Z}^m, A_{info}}^{\text{Action space}}, \overbrace{R, \zeta}^{\text{Reward function}}, \overbrace{\mathcal{P}, \mathcal{P}_0}^{\text{Transition functions}} \rangle$$

917 O is the set of possible observations in $[L_1, U_1] \times \dots \times [L_p, U_p] \times [L_1, U_1] \times \dots \times [L_p, U_p]$ where L_j
 918 is the minimum value of feature j over all data \mathbf{x}_i and U_j the maximum. $\mathbb{Z}^m \cup A_{info}$ is action space:
 919 actions can be label assignments in \mathbb{Z}^m or bounds refinements in A_{info} . The reward for assigning
 920 label $a \in \mathbb{Z}^m$ when observing some observation $\mathbf{o} = (L'_1, U'_1, \dots, L'_p, U'_p)$ is the proportion of
 921 training data satisfying the bounds and having label a : $R(\mathbf{o}, a) = \frac{|\{\mathbf{x}_i : L'_j \leq x_{ij} \leq U'_j \forall i, j\} \cap \{\mathbf{x}_i : y_i = a \forall i\}|}{|\{\mathbf{x}_i : L'_j \leq x_{ij} \leq U'_j \forall i, j\}|}$.
 922 The reward for taking an information gathering action that refines bounds is ζ . The transition func-
 923 tion is $\mathcal{P} : O \times (\mathbb{Z}^m \cup A_{info}) \rightarrow \Delta(O)$. When $a \in \mathbb{Z}^m$, $\mathcal{P}(\mathbf{o}, a, (L_1, U_1, \dots, L_p, U_p)) = 1$ (reset
 924 to full bounds). When $a = (k, v) \in A_{info}$, from $\mathbf{o} = (L'_1, U'_1, \dots, L'_p, U'_p)$, the MDP will transit
 925 to $\mathbf{o}_{left} = (L'_1, U'_1, \dots, L_k, v, \dots, L'_p, U'_p)$ (resp. $\mathbf{o}_{right} = (L'_1, U'_1, \dots, U'_k, v, \dots, L'_p, U'_p)$) with
 926 probability $\frac{|\{\mathbf{x}_i : L'_j \leq x_{ij} \leq U'_j \forall j \wedge x_{ik} \leq v\}|}{|\{\mathbf{x}_i : L'_j \leq x_{ij} \leq U'_j \forall j\}|}$ (resp. $\frac{|\{\mathbf{x}_i : L'_j \leq x_{ij} \leq U'_j \forall j \wedge x_{ik} > v\}|}{|\{\mathbf{x}_i : L'_j \leq x_{ij} \leq U'_j \forall j\}|}$).

927 Those classification POIBMDPs are essentially MDPs with stochastic transitions. It means that
 928 deterministic memoryless policies $O : \rightarrow A \cup A_{info}$ are in fact Markovian policy for those classi-
 929 fication POIBMDPs. More importantly, it means that, for a given γ and ζ , if we were to know the
 930 whole POIBMDP model, we could use planning, to compute *optimal* decision tree policies.